DISCLAIMER

This report was prepared as an account of work sponsored by an agency of the United States Government. Neither the United States Government nor any agency thereof, nor any of their employees, makes any warranty, express or implied, or assumes any legal liability or responsibility for the accuracy, completeness, or usefulness of any information, apparatus, product, or process disclosed, or represents that its use would not infringe privately owned rights. Reference herein to any specific commercial product, process, or service by trade name, trademark, manufacturer, or otherwise does not necessarily constitute or imply its endorsement, recommendation, or favoring by the United States Government or any agency thereof. The views and opinions of authors expressed herein do not necessarily state or reflect those of the United States Government or any agency thereof. Reference herein to any social initiative (including but not limited to Diversity, Equity, and Inclusion (DEI); Community Benefits Plans (CBP); Justice 40; etc.) is made by the Author independent of any current requirement by the United States Government and does not constitute or imply endorsement, recommendation, or support by the United States Government or any agency thereof.

LLNL-TR-2003434

Lawrence Livermore National Laboratory

Final Design for Additional Thermal/Epithermal eXperiments (TEX) with Sodium Chloride Absorbers to Provide Validation Benchmarks for TerraPower

More TEX-Cl Experimental Design Report

Eric Aboud

External (Unlimited)

March 12, 2025

Disclaimer

Acknowledgements

This work was supported by the Department of Energy (DOE)/Nuclear Regulatory Commission (NRC) Collaboration for Criticality Safety Support for Commercial-Scale HALEU for Fuel Cycles and Transportation (DNCSH), managed by Oak Ridge National Laboratory for the DOE.

This work is in collaboration with team members from Lawrence Livermore National Laboratory (LLNL), Los Alamos National Laboratory (LANL), and TerraPower.

Table of Contents

Section 1

Introduction

Overview

The first set of Thermal/Epithermal eXperiments (TEX) with chlorine absorbers (TEX-Cl) were executed in Q4FY24 and are in the process of being benchmarked for the ICSBEP. TEX-Cl builds upon the TEX-HEU baseline cases that were published in the 2022 International Criticality Safety Benchmark Evaluation Project (ICSBEP) Handbook [1]. TEX-HEU [2], like TEX-Pu, was designed to be modular to allow for the incorporation of various absorbers and reflectors to test nuclear data and application case needs. For example, TEX-HEU with hafnium (TEX-Hf) utilizes hafnium plates as both absorbers and reflectors, depending on the tested configuration. A second set of chlorine experiments, dubbed More TEX-Cl, are laid out in this report to meet the needs of TerraPower for chlorine validation for their Molten Chloride Fast Reactor (MCFR) systems.

TerraPower's Molten Chloride Reactor Experiment (MCRE) and MCFR are fast molten salt reactors that utilize sodium chloride (NaCl) salt eutectics as the fuel and coolant. The MCRE eutectic is a mixture of NaCl and uranium trichloride (UCl_3).

An abundant need for chlorine absorption validation has been expressed by multiple members of the community, including Y-12 (whose needs were addressed with the first set of experiments), LANL (whose needs were addressed with the Chlorine Worth Study (CWS)), TerraPower, institute de radioprotection et de sûreté nucléaire (IRSN), Savannah River Nuclear Solutions (SNRS), and others. Of the members who have expressed interest in this validation, most are interested in the fast neutron energy region, where the $^{35}Cl(n,p)$ reaction is most prominent. New $^{35}Cl(n,p)$ differential cross section measurements performed by LANL at LANCSE show substantial changes to the cross sections (Figure 1) and may be validated through these experiments as some configurations are optimally sensitive to this cross section.

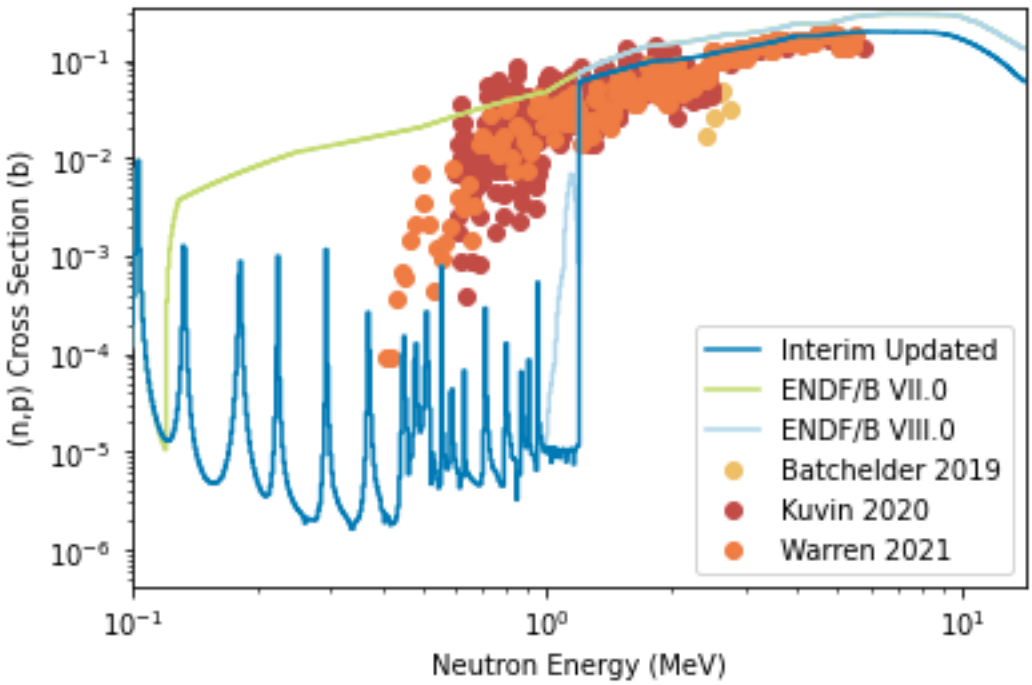

Figure 1: Comparison of Evaluated Nuclear Data to Experimental for $^{35}Cl(n,p)$[1].

The experimental design is akin to original TEX-Cl [3] configurations which utilized packed granular NaCl salt. The difference in this experiment is that the salt will be pressed, which allows for significantly higher densities, on the order of the theoretical density of the salt. Additionally, this experiment deviates from the previous design as it utilizes the Zeus [4] copper reflectors and 21" HEU plates for one configuration to achieve a maximally fast spectrum.

There is currently inadequate chlorine validation, with only two acceptable configurations in the ICSBEP handbook, and three additional configurations currently being analyzed for review into the ICSBEP handbook. This experiment, which describes three configurations, provides additional chlorine validation. The three identified configurations are based and built upon the final configurations of TEX-Cl. Two of the configurations were designed to maximize the similarity to the sensitivity profiles of the application cases provided by Idaho National Laboratory and TerraPower. The third configuration was designed to maximize the fast neutron capture sensitivity. To achieve the three configurations two absorber plate thicknesses are needed: 1/2" and 1" thick NaCl absorbers. The fastest configuration does not utilize polyethylene in the system and the other two configurations will need interstitial high-density polyethylene of thicknesses: 9/8" and 3/8". Detailed descriptions of the proposed configurations are provided in this document.

The largest assessed experimental uncertainty from non-absorber components is predicted to be of 0.00132 Δk_{eff}. The largest assessment of uncertainty resulting from the absorbers is predicted to be of 0.00042 Δk_{eff}. This results in a total uncertainty of 0.00139 Δk_{eff} for the copper-reflected assembly. The non-copper-reflected assembly is also expected to be bounded by this uncertainty. The largest contribution comes to uncertainty is the HEU plate gaps, which is manifested as the

[1] Via T. Cisneros *et al.* "Reactivity Impact of Updated 35Cl Nuclear Data on the Molten Chloride Reactor Experiment", presented at the International Conference on Physics of Reactors (PHYSOR) 2024 (2024).

core stack heights, which have been found to be reduced through coordinate measurement machine (CMM) measurements.

1.1 TerraPower and INL Needs

Idaho National Laboratory (INL) is working with TerraPower in the development of the Molten Chloride Reactor Experiment (MCRE). INL is the location for the MCRE tests as well as the salt eutectic fuel fabricator. The experiment is a critical fast-spectrum salt reactor utilizing molten chloride-based salts. Multiple criticality safety upset cases for the salt fuel fabrication were provided by INL [5] and are shown in Figure 2. The upset cases were compared to the sensitivity profiles discussed in this report and influenced the experimental design such that two of the three configurations were designed to be maximally similar to the INL sensitivity profiles. As MCRE ends and TerraPower transitions to the Molten Chloride Fast Reactor (MCFR) similar criticality safety considerations will exist, providing additional need for chlorine validation with cases that are as sensitive and similar to the upset conditions provided by INL.

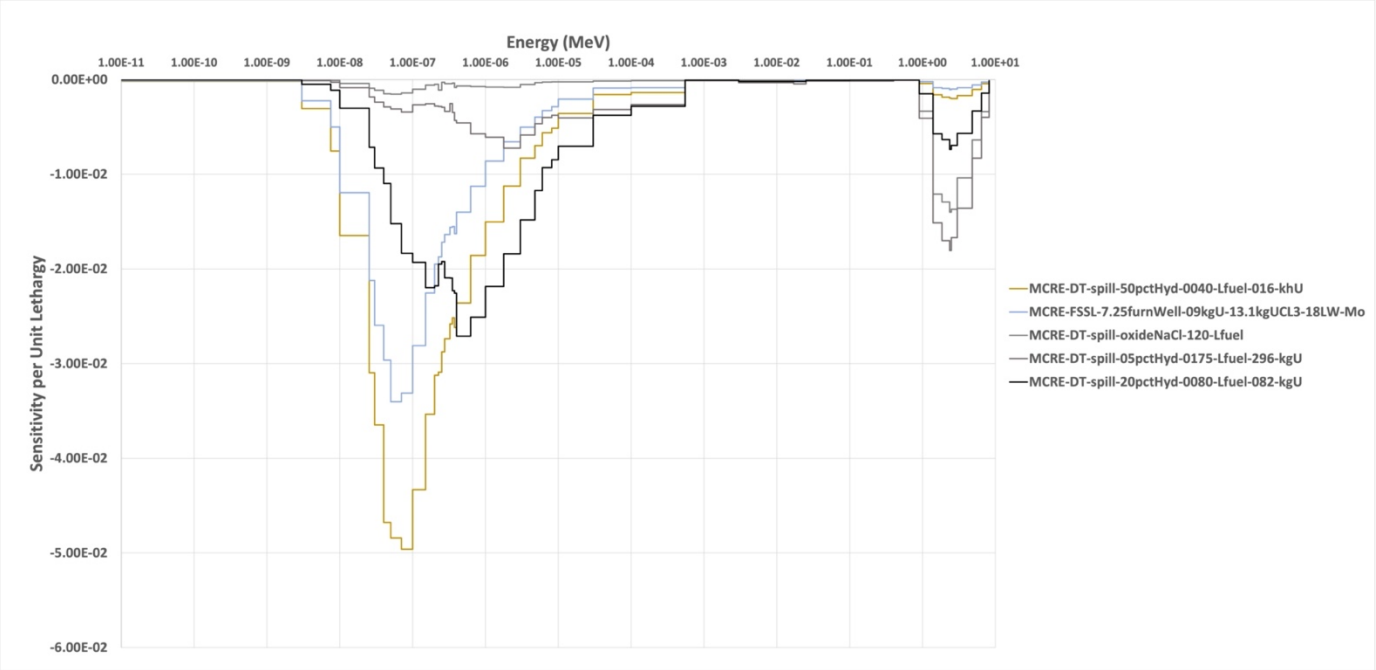

Figure 2: The Molten Chloride Reactor Experiment (MCRE) upset case sensitivity profiles.

MCRE is a physics experiment designed to collect data on fuel salt handling, approach to criticality, startup, fine reactivity control, shutdown, and inherent load-following capability. MCRE is a precursor to the MCFR, and as such is a much smaller reactor with different nuclear data needs, with the emphasis on a lower total mass with no power production. MCFR is a fast reactor whose fuel and coolant are NaCl eutectics. The fast reactor is highly sensitive to the ^{35}Cl(n,p) cross section, which has been known to be quite uncertain. The new differential cross

section measurements described in Section 1 are substantially different from the cross sections utilized in the current ENDF libraries. Calculations performed for MCRE with the new cross sections suggest a difference in reactivity of up to 2.2 percent in k_{eff} from ENDF/B-VII.0 and 0.9 percent in k_{eff} from ENDF/B-VIII.0[2].

[2] T. Cisneros *et al.* "Reactivity Impact of Updated 35Cl Nuclear Data on the Molten Chloride Reactor Experiment", presented at the International Conference on Physics of Reactors (PHYSOR) 2024 (2024).

Section 2

Equipment Description

In this discussion, Section 2.1 is directly taken from the IER-297 CED-4b previously conducted experiment [6] and both sections 2.2 and 2.4 are taken from IER-297-CED2 [7]. Section 2.3 is taken from [4]. Parts of Section 2 are taken from IER-499-CED3b [8].

2.1 Assembly Machine

The Comet General Purpose Critical Assembly Machine is a vertical lift machine (VLM) used to remotely assemble a critical experiment. As shown in Figure 3, Comet consists of the surrounding structure, stationary platform, and movable platen.

During assembly, roughly half of the experiment is built on the experiment platform with the other half on the lower adapter. During operation, the movable platen is extended vertically to bring the two halves of the experiment into contact. Once fully assembled, the two halves are only separated by a thin aluminum membrane.

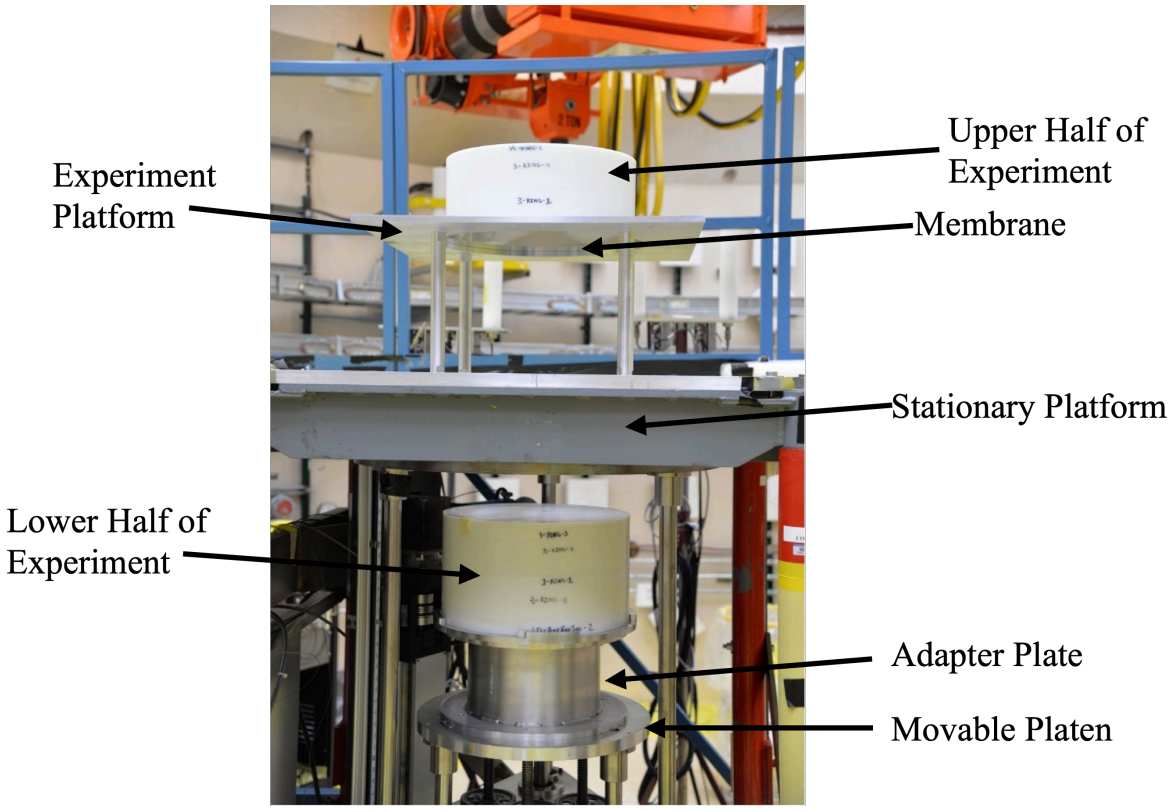

Figure 3: Comet General Purpose Critical Assembly Machine with additional TEX-HEU parts.

2.1.1 Stationary Platform

The experiment platform holds the upper half of the experiment, shown in Figure 4. The platform consists of an interface plate and four standoffs, which connect the interface plate to the stationary platform. The membrane is placed on top of the hole in the interface plate, allowing the movable platen to lift the upper half of the experiment as the lower half of the experiment pushes through the membrane. The interface plate includes four pegs to hold the membrane and alignment plate in place while still allowing vertical movement.

The interface plate is a 28” x 28”x 0.5” Al 6061-T6 plate with a 19” diameter hole through its center. The standoffs are varied lengths Al 6061-T6 cylinders with a 1.25” diameter. These standoffs affix the experiment platform to the stationary platform of Comet. The membrane is a 21 in x 21 in (53.34 cm x 53.34 cm) AL 6061-T6 plate with a thickness of 0.125 in (0.3175 cm). The membrane features four holes, one in each corner, ensuring consistent alignment when placed onto the interface plate using the four pegs. The design allows the membrane to be lifted to 0.75 in (1.905 cm).

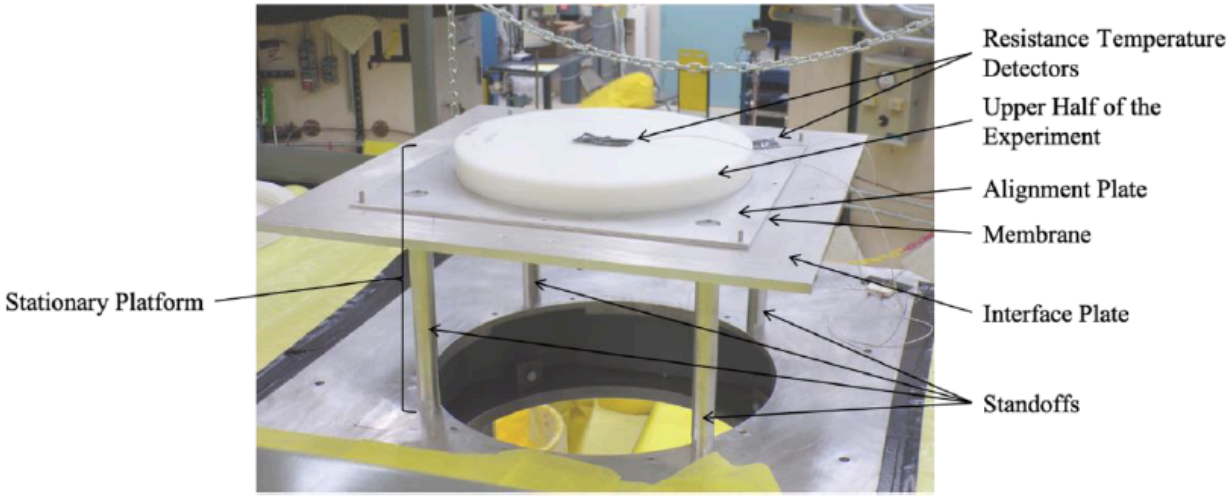

Figure 4: Experiment platform, Alignment Plate, and Membrane on the Stationary Platform of Comet.

2.1.2 Movable Platen

The lower adapter holds the lower half of the experiment, shown in Figure 5. This lower adapter consists of an adapter plate and an adapter extension, which affixes the lower adapter to the movable platen. An updated adapter plate was designed to allow for access to the source holder of the new bottom reflector plates. The adapter plate has an outer diameter of 18.5 in (46.99 cm) and a thickness of 0.53 in (1.3462 cm). This plate features a 17.150 in (43.561 cm) inner diameter with an additional 0.47 in (1.1938 cm) lip height to hold the bottom polyethylene reflector plate. The difference between the old and new design is that the new design minimizes the lip surface area, reducing the size of the lips to provide easier access to the bottom reflector plate. The adapter extension is an 8 in (20.32 cm) tall annular cylinder with a wall thickness of 0.25 in (0.635 cm) and a 12 in (30.48 cm) outer diameter. This extension includes a 2.5 in (6.35 cm) wide and 0.5 in

(1.27 cm) thick top and bottom lip to affix it to the adapter plate and the platen. Both components of the lower adapter are Al 6061-T6. Figure 5 shows the movable platen with the old adapter plate, Figure 6 shows the new adapter plate design, and Figure 7 shows a drawing of the updated lower adapter design.

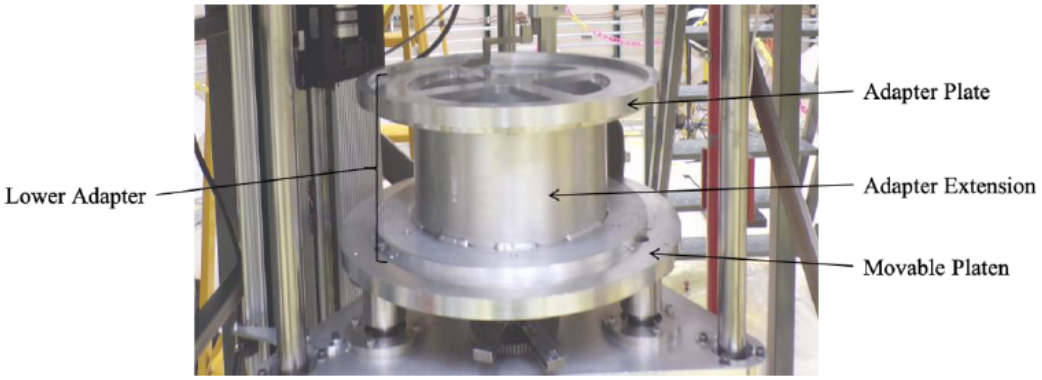

Figure 5: Lower Adapter on the Movable Platen of Comet.

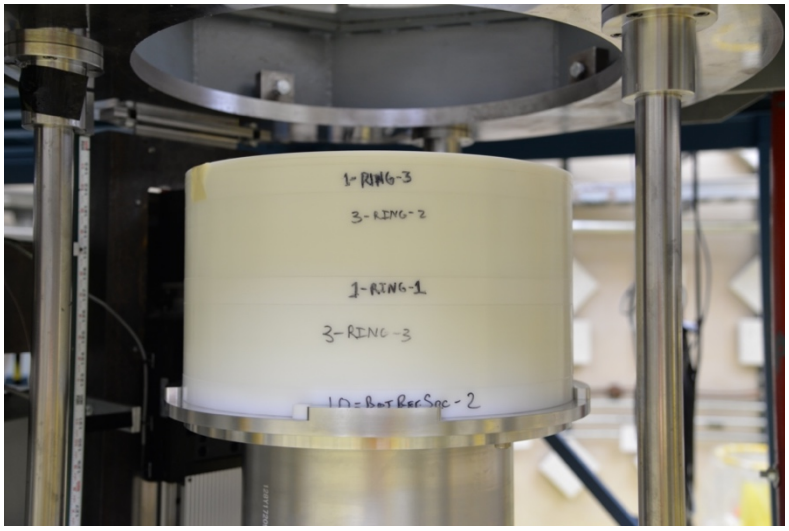

Figure 6: Lower platen with the new adapter plate, which highlights the difference between the lip design of the new and old design.

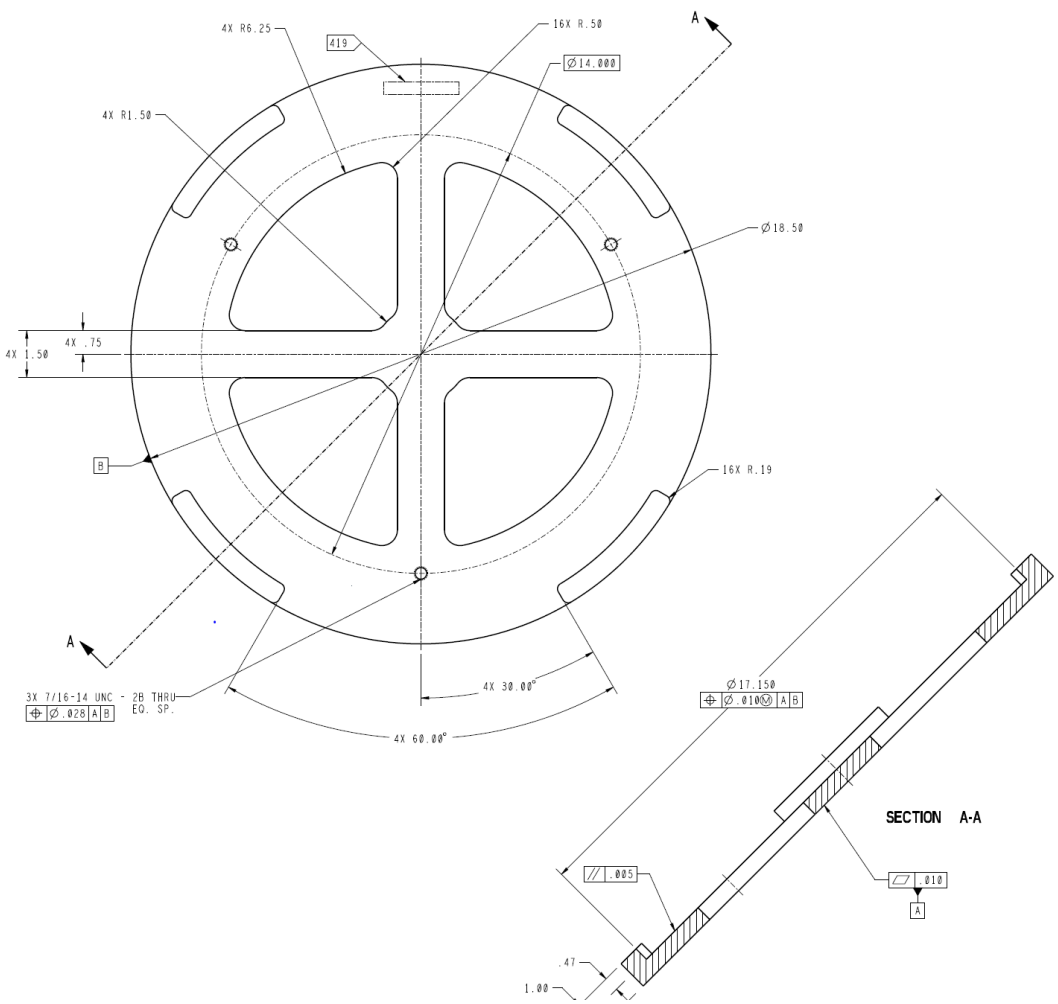

Figure 7: Drawing of the updated lower adapter plate.

2.2 Highly Enriched Uranium Plates

Los Alamos National Laboratory (LANL) has used thin (3 mm thickness) solid and annular disks of U(93+), collectively known as the Jemima plates, in many critical experiments. Solid 15-inch diameter plates along with similar plates with a 2.5-inch diameter central hole were manufactured by LANL in the mid-1950s and used in the Jemima experiments (IEU-MET-FAST-002) [13]. Some of the original 15-inch plates were modified with 6 and 10 inch diameter central holes for the series of Big Ten experiments at LANL [15]. Additionally, 21-inch outer diameter and 15-inch inner diameter plates were fabricated. The Jemima plates have also been used to create intermediate spectra benchmarks in the Zeus experiments [15-17].

NCERC has a total of 31 of the 21-inch plates which all have outer diameters of 21-inches and inner diameters of 15-inches [18]. The available inventory for the 15-inch and 21-inch plates is shown in Table 1. The current 15-inch OD plate inventory is made up of the equivalent of 7 solid plates, 7 2.5-inch ID plates, 5 6-inch ID plates, and 8 10-inch ID plates. One of the 7 solid plate

equivalents is made up of 6 wedges and one of them is made up of the combination of a 6-inch ID plate and a solid 6-inch OD plate. The masses and dimensions of these plates are taken from four separate sources [14, 16-17,19] and the total HEU mass available in the 15-inch OD Jemima plates is 145.6 kg so experimental configurations requiring more than this mass are not possible unless additional HEU plates are fabricated. There is also one extra 6-inch ID plate (Inventory ID 10493, mass 5441) for which the enrichment has not been found, so it was not included in this analysis.

Table 1: 15" and 21" OD Jemima Plate Dimensions, Mass, and Enrichment.

Mat. ID	Plate Type	Inventory ID	Inner D, in	Outer D, in	Thickness, in	Mass, g	U235 wt%
m3	Solid	11147	-	15	0.11[a]	6539[b]	93.17[b]
m4	Solid	11017	-	15	0.119[a]	6518[b]	93.31[b]
m5	Solid	11019	-	15	0.124[a]	6477[b]	93.18[b]
m6	Solid	11150	-	15	0.118	6441[b]	93.17[b]
m7	Solid	11149	-	15	0.118[a]	6412[b]	93.24[b]
m8	6-inch hole	B1010457	6.005	15	0.118	5575[c]	93.44[c]
m9	2.5-inch hole	B1010491	2.51	15	0.122[a]	6396[b]	93.37[b]
m10	2.5-inch hole	B1010489	2.51	15	0.118	6350[b]	93.39[b]
m11	2.5-inch hole	B1010467	2.51	15	0.116[a]	6337[b]	93.41[b]
m12	2.5-inch hole	B1010470	2.51	15	0.118	6291[b]	93.41[b]
m13	2.5-inch hole	10487	2.51	15	0.118	6277[b]	93.26[b]
m14	2.5-inch hole	10464	2.51	15	0.114[a]	6259[b]	93.38[b]
m15	2.5-inch hole	B1010475	2.51	15	0.118	6244[b]	93.4[b]
m16	6-inch hole	B1010477	6.005	15	0.118	5511[c]	93.35[c]
m17	6-inch hole	B1010935	6.005	15	0.118	5444[c]	93.16[c]
m18	6-inch hole	10933	6.005	15	0.111[a]	5442[b]	93.16[b]
m19	6-inch hole	B1010932	6.005	15	0.118	5440[b]	93.15[b]
m20	6-inch hole	B1011018	6.005	15	0.118	5378[b]	93.19[b]
m21	10-inch hole	B1010463	10.005	15	0.118	3633[c]	93.41[c]
m22	10-inch hole	B1010458	10.005	15	0.118	3619[c]	93.4[c]
m23	10-inch hole	-	10.005	15	0.118	3610[c]	93.41[c]
m24	10-inch hole	-	10.005	15	0.118	3610[c]	93.24[c]
m25	10-inch hole	B1010481	10.005	15	0.118	3595[c]	93.23[c]
m26	10-inch hole	B1010472	10.005	15	0.118	3594[c]	93.5[c]
m27	10-inch hole	B1010479	10.005	15	0.118	3566[c]	93.3[c]

m28	10-inch hole	B1010483	10.005	15	0.118	3546[c]	93.24[c]
m29	Wedges	8601-8606	-	15	0.118	6446[b]	93.13[b]
m30	6-inch piece	Q2-16	-	6	0.118	1078[b]	93.14[b]
-	21-inch plate	Average	15	21	0.118	6118[d]	93.16[d]

[a] The thicknesses of these plates were measured with calipers and reported to a precision of 0.001 inches. Three measurements were taken of each of these plates and the average reported. The rest of the plate thicknesses in the table are reported as the nominal value of 0.118 inches [17]

[b] Values reported in HEU-MET-FAST-072 [16]

[c] Values reported in IEU-MET-FAST-007 [14]

[d]Average of the values reported in HEU-MET-INTER-011 [##]

The column labeled Material ID in Table 1 refers to the material number assigned to the plate in Monte Carlo models for this report. Each plate is assigned a number between 3 and 30 in order of decreasing plate mass (with exceptions for m8 and m29).

Tolerances for the outer diameters and thicknesses of the Jemima plates are +0.000/-0.005 in, and ±0.002 in, respectively [16]. The tolerance for the inner diameter of the 2.5-inch hole plates is +0.005/-0.000 in [17]. According to reference [11], drawings for the 6-inch hole and 10-inch hole plates could not be located, so tolerances on their inner diameters are not known. Inner and outer diameters of the Jemima plates are reported as nominal dimensions.

The masses and ^{235}U enrichment values were measured individually for every plate [10,11]. IEU-MET-FAST-007 [14] and HEU-MET-FAST-072 [16] report the ^{235}U enrichment values to a precision of 0.01 wt%. The relative abundances of uranium isotopes were reported for four of the 15-inch OD plates and one 21-inch OD plate, as shown in Table 2 [14,16].

Table 2: Relative Abundances of Uranium Isotopes in Jemima Plates.

Type	Inventory ID	Uranium Isotope Atomic Ratio			
		^{234}U	^{235}U	^{236}U	^{238}U
6-inch hole	B1010932	(1.08±0.01)e-2	1	(3.50±0.04)e-3	(5.86±0.02)e-2
	B1011018	(1.10±0.01)e-2	1	(5.65±0.06)e-3	(5.55±0.02)e-2
10-inch hole	10458	(1.11±0.02)e-2	1	<2e-5	(5.77±0.02)e-2
15-inch plates	10493	(1.15±0.01)e-2	1	(8.40±0.42)e-4	(5.92±0.02)e-2
21-inch plates	B-2444-13	(1.06±0.01)e-2	1	(4.63±0.05)e-3	(5.67±0.02)e-2

The elemental impurities were measured for five of the 15-inch OD Jemima plates and the 21-inch OD plates, as shown in Table 3 [16].

Table 3: Jemima Plate Impurity Content

Plate Type		Solid	Solid	Solid	6-inch hole	6-inch hole	21-inch Plate
Inventory ID		11147	11149	11150	B1010932	10933	Average
Impurity (ppm)	Li	<0.1	<0.1	<0.1	<0.1	<0.1	<0.1
	Be	<0.1	<0.1	<0.1	<0.1	<0.1	<0.02
	B	0.6	0.6	0.3	0.2	<0.1	0.5
	C	1100	270	320	170	170	441
	Na	<1	<1	<1	<1	<1	<1
	Mg	<1	<1	<1	<1	1	<1
	Al	50	40	20	150	100	32
	Si	300	400	210	80	130	256
	Ca	<2	<2	<2	<2	<2	<5
	V	<20	<20	<20	<20	<20	1
	Cr	5	15	5	2	3	7
	Mn	4	7	6	7	6	5
	Fe	100	190	90	70	30	179
	Co	<5	<5	<5	<5	<5	1
	Ni	20	30	20	15	15	27
	Cu	6	5	4	4	3	7
	Mo	50	<25	<25	-	-	86
	Sn	<1	<1	<1	-	-	<1
	Pb	5	<1	<1	-	-	<1

2.3 Copper Reflectors

A deviation from the original TEX-Cl is the inclusion of the Zeus copper reflectors. The copper reflectors were manufactured at Asarco and delivered to LANL over multiple years. The reflectors include top, bottom, corner, and side reflectors. The top, bottom, and side reflectors arrived in 1996. Some of the corner reflectors arrived in 1996 (corner reflectors with nominal heights 5.68, 3.00, 1.50, 0.75, and 0.375 inches) and others arrived in 2001 (corner reflectors with nominal heights of 0.25 and 0.187 inches).

The side reflector stack is made up of the side reflectors which act as the outer surface of the reflector with the corner reflectors interior to the side reflectors, see Figure 8. At the top of the

reflector stack, the upper reflector piece will sit on top of the highest four corner reflector pieces. The four lowest corner reflectors of the upper stack have additional bolt holes so that they can be secured to the top plate. The bolt holes will be filled with copper bolts of unknown mass.

The drawing dimensions of the corner reflector parts are shown in Table 4. The drawing dimensions of the top and side reflectors are shown in Table 5. The drawing dimensions of the bottom reflector are shown in Table 6. The measured masses of the copper reflector pieces are shown in Table 7. The copper reflector impurities are shown in Table 8. For the purposes of this report the copper was assumed to be pure.

Figure 8: Example of the copper reflectors with the side reflectors and three corner reflectors installed.

Table 4: Copper corner reflector drawing dimensions.

Part Height ID	Outside Length		Inside Radius		Height	
	[in (cm)]	Tolerance [in (cm)]	[in (cm)]	Tolerance [in (cm)]	[in (cm)]	Tolerance [in (cm)]
0.187 in	11.00 (27.94)	+0.000,-0.01 (+0.000,-0.0254)	10.55 (26.797)	±0.01 (±0.0254)	0.187 (0.47498)	±0.005 (±0.0127)
0.250 in					0.250 (0.635)	±0.005 (±0.0127)
0.375 in					0.375 (0.9525)	±0.005 (±0.0127)
0.75 in					0.75 (1.905)	±0.01 (±0.0254)
1.50 in					1.50 (3.81)	±0.01 (±0.0254)
3.00 in					3.00 (7.62)	±0.01 (±0.0254)
5.68 in					5.68 (14.4272)	±0.01 (±0.0254)

Table 5: Copper side and top reflector drawing dimensions.

Part	Length		Width		Height	
	[in (cm)]	Tolerance [in (cm)]	[in (cm)]	Tolerance [in (cm)]	[in (cm)]	Tolerance [in (cm)]
Copper Bottom Side Reflector	28.38 (72.0852)	±0.01 (±0.0254)	6.38 (16.2052)	±0.01 (±0.0254)	8.13 (20.6502)	±0.01 (±0.0254)
Copper Side Reflector	28.38 (72.0852)	±0.01 (±0.0254)	6.38 (16.2052)	±0.01 (±0.0254)	8.13 (20.6502)	±0.01 (±0.0254)
Copper Top Reflector	22.00 (55.88)	+0.00, -0.01 (+0.000, -0.0254)	22.00 (55.88)	+0.00, -0.01 (+0.000, -0.0254)	5.68 (14.4272)	±0.01 (±0.0254)

Table 6: Copper bottom reflector drawing dimensions.

Part	Inner Diameter		Outer Diameter		Height	
	[in (cm)]	Tolerance [in (cm)]	[in (cm)]	Tolerance [in (cm)]	[in (cm)]	Tolerance [in (cm)]
Copper Bottom Reflector	2.50 (6.35)	±0.01 (±0.0254)	21.00 (53.34)	±0.01 (±0.0254)	5.68 (14.4272)	±0.01 (±0.0254)

Table 7: Measured masses of each of the copper reflector pieces.

Part Type	Height[(a)] [in (cm)]	Average Mass of Components[(b)] [*as defined*]
Copper Top Reflector	5.68 (14.4272)	395.6 kg
Copper Bottom Reflector	5.68 (14.4272)	616 lbs
Copper Corner Reflector	5.68 (14.4272)	60.2 lbs
	3.00 (7.62)	14390.5 g
	0.75 (1.905)	3560.6 g
	1.50 (3.81)	7143.9 g
	0.187 (0.47498)	905.8 g
	0.250 (0.635)	1060.9 g
	0.375 (0.9525)	1797.9 g
Copper Side Reflectors	8.13 (20.6502)	464.4 lbs

[(a)]Dimensions from drawings.

[(b)]Physical measurements via one of three scales that read out grams, kilograms, or pounds.

Table 8: Copper Reflector Impurities (ppm except oxygen in wt-%).[a]

Element		Copper Reflector Impurities (ppm)	
		Cast # 60434	Cast # 60472
Impurity (ppm)	Sb	0.8	1.1
	As	0.4	0.1
	Bi	0.4	0.5
	Fe	4.4	3.2
	Pb	1.3	0.6
	Ni	3.0	1.0
	Se	0.2	0.2
	Ag	11.0	16.0
	Te	0.1	0.1
	Sn	0.2	0.1
	Zn	0.3	0.1
	O (wt-%)	0.046	0.036

[a]R.P. Damjanovich, "ASARCO Copper Order for the Zeus Experiments" Los Alamos National Laboratory memorandum NIS6-96:0314RPD, June 24, 1996.

2.4 Polyethylene Reflectors and Moderators

For the two thermal configurations which do not utilize the copper reflectors, the assembly is surrounded by a 1-inch-thick high-density polyethylene (HDPE) reflector composed of one plate on the top and one on the bottom as well as a stack of cylindrical shells around the sides. The polyethylene reflector on the top of the assembly, as well as the moderator plates, is a cylinder with an outer diameter of 15 inches. The thickness of the top reflector can be increased to 2 inches in increments of 1/16 inch to increase reactivity of the assembly. The 1-inch-thick reflector around the side of the assembly is made up of stacked cylinders with 15.1-inch inner diameter, 17.1-inch outer diameter, and various heights ranging from 1/32 inch to 3 inches, as shown in Table 9. Additional HDPE reflector pieces can be procured if needed. The 3-inch-tall cylinders will be added first as the assembly is stacked, with the smaller cylinders used to precisely adjust the reflector height to match the inner height of TEX core stack to within the nearest 1/32-inch.

To ensure that the assembly remains centered throughout the experiment, and to provide extra stability, the cylindrical reflectors have stacking step joints on their top and bottom, as shown in Figure 9.

Table 9: HDPE Reflector and Moderator Parts

Part Name	Quantity
3" HDPE Reflector Ring	5
1" HDPE Reflector Ring	9
1/2" HDPE Reflector Ring	4
1/4" HDPE Reflector Ring	4
7/32" HDPE Reflector Cap	2
5/32" HDPE Reflector Cap	1
1/16" HDPE Reflector Cap	1
1/32" HDPE Reflector Cap	2
0" HDPE Reflector Cap	3
Bottom Reflector Cap (See Figure 13)	3
1/8" HDPE Moderator	18
3/4" HDPE Moderator	16
11/16” HDPE Moderator	14
1” HDPE Moderator	11
Bottom Reflector	3
1" HDPE Reflector Plate	3
1/16" HDPE Reflector Plate	2

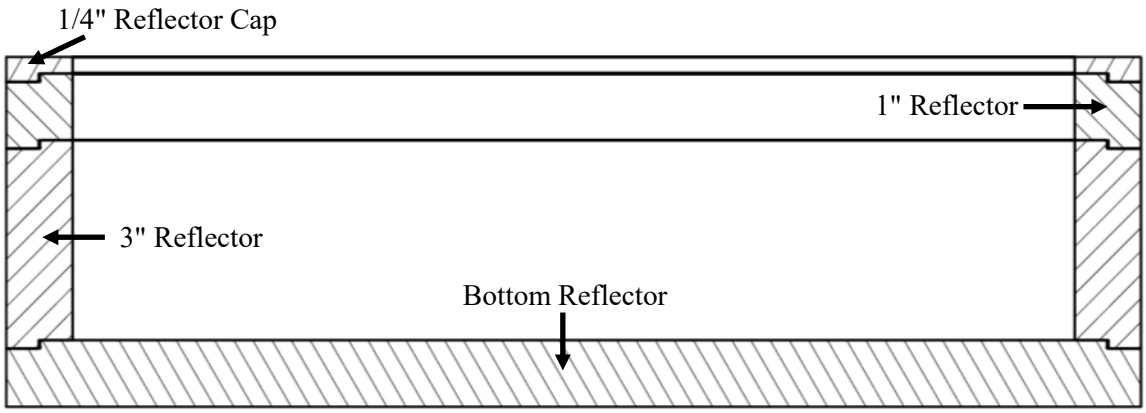

Figure 9: Cross Sectional View of an example 5.25" Reflector Assembly for Bottom Half.

The bottom reflector has a 17.1-inch OD and a step joint into which the first 3-inch cylindrical reflector part fits. A cavity exists to contain the source, which allows for easy installation and removal without the need for restacking the configuration. The configurations are assembled by first stacking the HEU, moderator, and absorber plates to a height of 3 inches on top of the bottom reflector, then lowering the first 3-inch reflector around the stack. The process is then repeated, using the 3-inch, 1-inch, 1/2-inch, and 1/4-inch reflectors as needed until the stack is within 1/4

inch of the height of the bottom half of the assembly. Then the appropriate reflector cap is used to adjust the reflector height to the nearest 1/32 inch. The reflector caps have a step joint on the bottom but are flat on the top so that the top of the sidewall reflector is flush with the top of the inner TEX stack.

The top half of each assembly requires a slightly different set of reflectors, as shown in Figure 10. Instead of the bottom reflector part, the base of the top half of the assembly is composed of the 3-inch reflector part and the 0-inch bottom cap part, which simply fills in the step joint. The top half of the assembly requires an extra 1-inch reflector to reach the same stack height as the bottom assembly, since the top reflector sits inside the side wall reflectors and does not add an inch to the height like the bottom reflector does.

Most of the reflector components were procured for the IER-499 experimental campaign. Interstitial moderator thicknesses of 3/8” and 1” are needed, however 1” plates are already being procured for another campaign. Only the new 3/8” moderator plates need to be procured. Additional polyethylene may be procured as needed.

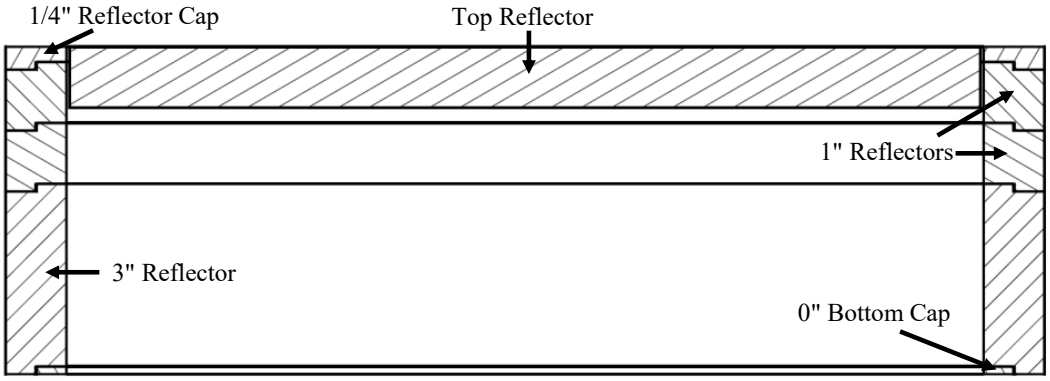

Figure 10: Cross Sectional View of an example 5.25-Inch Reflector Assembly for Top Half.

2.5 Sodium Chloride (NaCl) Plate Description

High-purity sodium chlorine salts (NaCl) will be used in the More TEX-Cl experiments as the source of chlorine. The NaCl salt selected for these experiments was identified due to its purity with only trace impurities, seen in Table 10 for the previous TEX-Cl experiment. NaCl contains 60.67% Cl by weight and is an abundant, lowly desiccating salt with a packing density of 1.217 g/cm^3 [9] and a theoretical density of 2.16 g/cm^3 [10]. In previous experiments the salt was found to have a water content of ~160 ppm. It should also be noted that sodium has a significantly lower thermal neutron capture cross section than chlorine. It is estimated that a density of 90% theoretical (1.944 g/cm^3) is achievable through pressing techniques. NaCl salt will be pressed in half plates then assembled within aluminum tins.

Table 10: Measured NaCl impurities.

Element	Concentration [ppm wt]			
	01-08	01-10	01-11	01-13
Li	0.01	<0.01	<0.01	<0.01
Be	<0.01	<0.01	<0.01	<0.01
B	<0.05	<0.05	<0.05	<0.05
C	-	-	-	-
N	-	-	-	-
O	-	-	-	-
F	<1	<1	<1	<1
Na	Matrix	Matrix	Matrix	Matrix
Mg	0.86	0.47	0.39	0.47
Al	0.05	0.18	<0.05	0.07
Si	0.07	0.33	<0.05	0.12
P	<0.1	<0.1	<0.1	<0.1
S	1.2	5.1	3.4	3.1
Cl	Matrix	Matrix	Matrix	Matrix
K	4.3	7.8	14	17
Ca	0.9	2.1	2	1.6
Sc	<0.01	<0.01	<0.01	<0.01
Ti	<0.05	<0.05	<0.05	<0.05
V	<0.05	<0.05	<0.05	<0.05
Cr	<0.05	<0.05	<0.05	<0.05
Mn	<0.05	<0.05	<0.05	<0.05
Fe	<0.1	<0.1	<0.1	<0.1
Co	<0.05	<0.05	<0.05	<0.05
Ni	<0.1	<0.1	<0.1	<0.1
Cu	<1	<1	<1	<1
Zn	<0.1	<0.1	<0.1	<0.1
Ga	<0.05	<0.05	<0.05	<0.05
Ge	<0.5	<0.5	<0.5	<0.5
As	Interference	Interference	Interference	Interference
Se	<0.5	<0.5	<0.5	<0.5
Br	2.7	12	16	13
Rb	<0.01	<0.01	<0.01	<0.01
Sr	<0.12	<0.19	<0.11	<0.23
Y	<0.01	<0.01	<0.01	<0.01
Zr	<0.05	<0.05	<0.05	<0.05

Element	Concentration [ppm wt]			
	01-08	01-10	01-11	01-13
Nb	<50	<50	<50	<50
Mo	<20	<20	<20	<20
Ru	<0.05	<0.05	<0.05	<0.05
Rh	<5	<5	<5	<5
Pd	<0.05	<0.05	<0.05	<0.05
Ag	<0.1	<0.1	<0.1	<0.1
Cd	<0.1	<0.1	<0.1	<0.1
In	<1	<1	<1	<1
Sn	<0.1	<0.1	<0.1	<0.1
Sb	<0.05	<0.05	<0.05	<0.05
Te	<0.05	<0.05	<0.05	<0.05
I	<0.05	<0.05	<0.05	<0.05
Cs	<0.5	<0.5	<0.5	<0.5
Ba	<0.05	<0.05	<0.05	<0.05
La	<0.05	<0.05	<0.05	<0.05
Ce	<0.05	<0.05	<0.05	<0.05
Pr	<0.05	<0.05	<0.05	<0.05
Nd	<0.05	<0.05	<0.05	<0.05
Sm	<0.05	<0.05	<0.05	<0.05
Eu	<0.05	<0.05	<0.05	<0.05
Gd	<0.05	<0.05	<0.05	<0.05
Tb	<0.05	<0.05	<0.05	<0.05
Dy	<0.05	<0.05	<0.05	<0.05
Ho	<0.05	<0.05	<0.05	<0.05
Er	<0.05	<0.05	<0.05	<0.05
Tm	<0.05	<0.05	<0.05	<0.05
Yb	<0.05	<0.05	<0.05	<0.05
Lu	<0.05	<0.05	<0.05	<0.05
Hf	<0.5	<0.5	<0.5	<0.5
Ta	Electrode	Electrode	Electrode	Electrode
W	<5	<5	<5	<5
Re	<0.1	<0.1	<0.1	<0.1
Os	<0.01	<0.01	<0.01	<0.01
Ir	<0.01	<0.01	<0.01	<0.01
Pt	<0.05	<0.05	<0.05	<0.05
Au	<5	<5	<5	<5
Hg	<0.1	<0.1	<0.1	<0.1

Element	Concentration [ppm wt]			
	01-08	01-10	01-11	01-13
Tl	<0.01	<0.01	<0.01	<0.01
Pb	<0.05	<0.05	<0.05	<0.05
Bi	<0.01	<0.01	<0.01	<0.01
Th	<0.005	<0.005	<0.005	<0.005
U	<0.005	<0.005	<0.005	<0.005

The encapsulation containers are custom designed in aluminum for the experiment and are cylindrical disks with the same diameter as the HEU plates, 15” diameters. Figure 11 shows a drawing of the NaCl plates for the IER-499 TEX-Cl experiment which used a 12” inner diameter. For the configuration that utilizes the 21” HEU plates an aluminum ring of the same thickness as the NaCl plates will be used to fill the difference. The tin thicknesses were designed so that there was one set of 1/2”-thick and one set of 1”-thick cavities. Both sets of plates have a 1/8”-thick bottom and a 1/16”-thick top. The active absorber diameter is 14” with the remaining 1” being aluminum to match the overall diameter of the 15” HEU plates with an optional 6” aluminum ring to match the overall diameter of the 21” HEU plates. A 3” inner annulus may be introduced to the absorber plate design to allow for the alignment tube for the Zeus-like configuration. The bottom section is a solid machined part while the top “lid” is fastened via sixteen Al-2024 screws. A retaining lip was designed in the base component to assist in the attachment of the lid but also provides a soldering cavity if air tightness is not achieved with the fasteners. The NaCl discs will be fabricated externally and will be placed into the tins after fabrication. The mass of the salt will be precisely known as it will be measured during the filling of the containers.

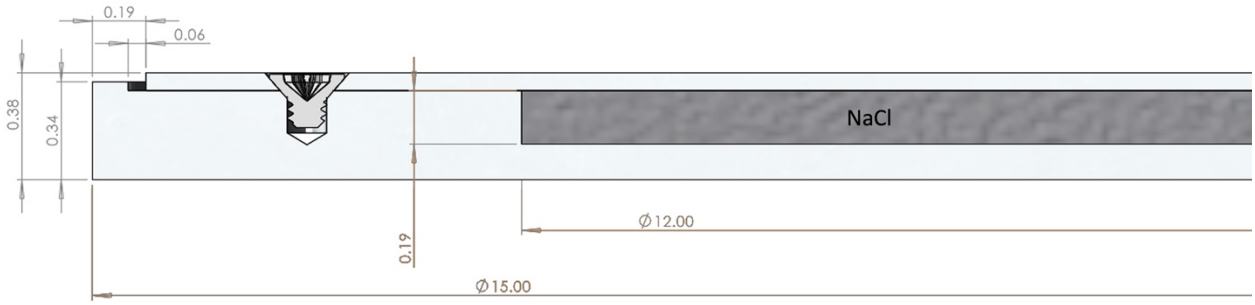

Figure 11: Cut CAD drawing of the TEX-Cl 3/16” NaCl absorber with encapsulation, as an example. Only the edge of the plate is shown.

2.6 Experimental Configurations

The experimental configurations identified in this study are similar to the original TEX-HEU configurations from IER-297 [6]. The critical assemblies will be composed of stacks of HEU plates with varying thicknesses of interspersed high-density polyethylene (HDPE) moderator and NaCl plates. Two assemblies will be enclosed in 1” of polyethylene reflectors on the bottom and sides, with variable upper reflector thicknesses. One assembly will utilize the Zeus copper reflectors above, below, and surrounding the assembly. All configurations follow the standard stacking

model. The specific configurations described in this report, including which plates are used and their order of stacking, are meant to be best estimates for what the critical configurations will be.

The standard stacking model is made up of a repeating pattern of one HEU plate, one moderator plate, and one absorber plate as seen in Figure 12. The pattern is broken on the top layer as there is no absorber plate or moderator plate between the last HEU plate and the upper reflector. Figure 13 shows the Zeus-like configuration.

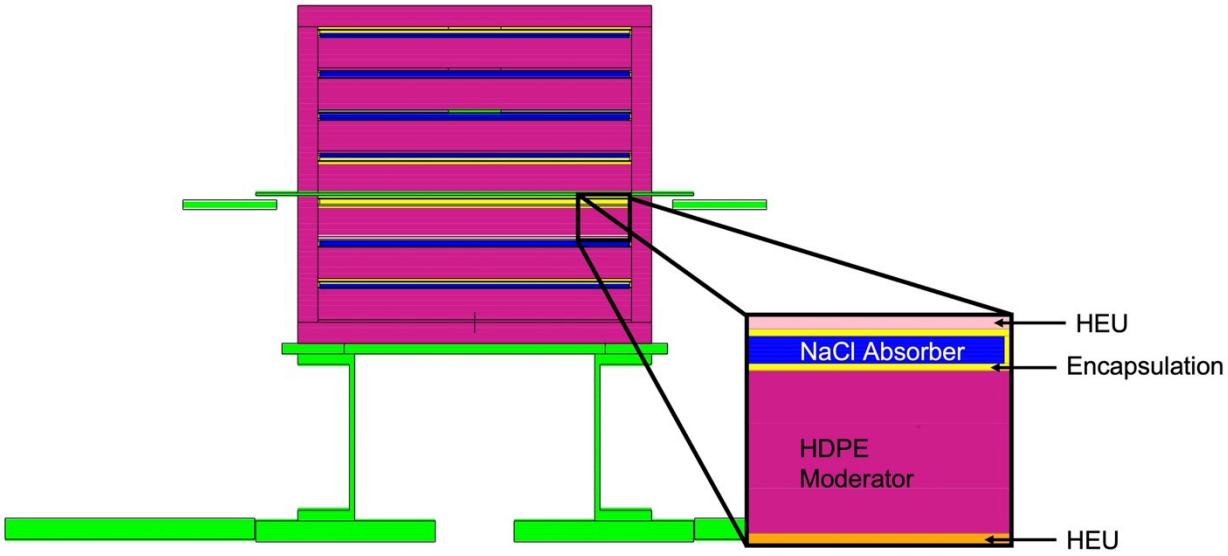

Figure 12: Standard stacking configuration for the polyethylene moderated and reflector configurations. A single unit consists of a layer of polyethylene moderator (pink), an absorber material (blue), and a HEU plate (orange).

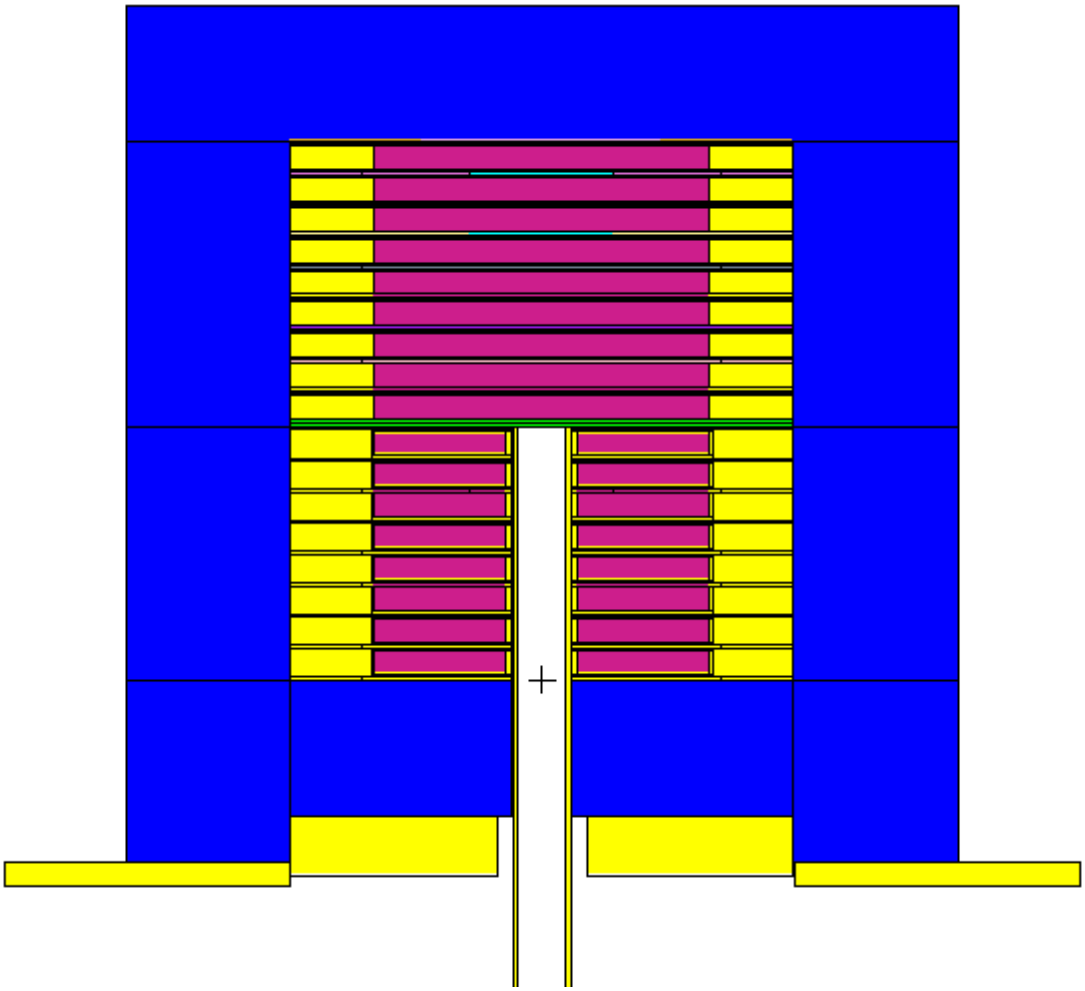

Figure 13: Standard configuration for the Zeus-like assembly. The central alignment tube goes through the center of the lower stack to ensure alignment of the plates.

Section 3

Calculational Models of the Experiments

3.1 Methodology and Code Used

The Monte Carlo neutron transport code, MCNP6® [19,20], developed at Los Alamos National Laboratory, was used to calculate neutron multiplication, neutron spectrum, sensitivity to variations in cross section data, and the uncertainty and bias in the models for each experimental configuration. Continuous energy ENDF/B-VIII.0 cross sections were used in all MCNP6.2® calculations. All materials were modeled using room temperature (293 K) cross sections.

Each HEU plate was modeled individually using reported values where possible. The ^{235}U content has been measured for each plate, so individual values for each plate were included in the model. However, the relative abundance of other uranium isotopes was only measured for three plates, so average values of 1.032 wt% ^{234}U and 0.234 wt% ^{236}U were used for all other HEU plates, with the remainder of the uranium content being ^{238}U. The elemental impurities were only measured for five Jemima plates. An average of these values for each elemental impurity was used for the rest of the HEU plates.

While the thicknesses of several HEU plates were measured, all plates were modeled with their nominal thickness of 0.118 inches. The mass of each plate was measured and individually included in the model. The absorber components have not yet been fabricated and all dimensions are nominal. The density of NaCl was taken to be 1.944 g/cm^3, and the aluminum encapsulation was taken to be 2.7 g/cm^3. The density of the polyethylene moderators and reflector is modeled as 0.967 g/cm^3. The density of the copper reflectors is taken to be 8.96 g/cm^3. The models include the aluminum or steel membrane, upper stationary platform, and the Comet vertical lift machine. Bias inherent to the calculations due to modeling the experimental configurations in a vacuum and excluding the effects of room return is described in Section 3.4.

The non-default parameters used for eigenvalue calculations are listed in Table 11. The sensitivity calculations were evaluated using the MCNP6 KSEN functionality card over three types of energy structures. One set of calculations was done using the 3-group energy structure for thermal range [0 MeV – 0.625E-6 MeV], intermediate range [0.625E-6 MeV-0.1 MeV], and fast range [0.1 MeV – 20 MeV]. Tallies with a SCALE 44-group structure were run to compare to INL provided sensitivity profiles [21].

Table 11: Parameters used in MCNP6® calculations.

Parameter	Value
Number of generations run	2000
Number of neutrons started per generation	100,000
Number of generations skipped	500

3.1.1 MCNP Models of Absorber Materials

The absorber layers in the experiment are aluminum encapsulated NaCl salts (Table 12). To estimate the structure of the absorber assemblies, the absorber volume was surrounded by solid aluminum of the same thicknesses as reality. The total diameter of the plates are 15 inches with the active absorber diameters being 12 inches. Two thicknesses, 1/2" and 1" thick, plates were modeled with pure NaCl (density of 1.944 g/cm^3). The encapsulation was taken to be pure Aluminum 6061 (density of 2.7 g/cm^3) with a 1.5 inch radially thick solid ring around the perimeter for the 15" plates or a 7.5 inch radially thick solid ring around the perimeter for the 21" plates, a 1/16" top plate, and a 1/8" bottom plate. Figure 14 shows the MCNP model of the TEX-Cl 3/16" absorber plate and encapsulation.

Table 12: Composition of an NaCl absorber.

Element/Isotope	^{35}Cl	^{37}Cl	^{23}Na
Atomic Percent	37.88	12.12	50.00

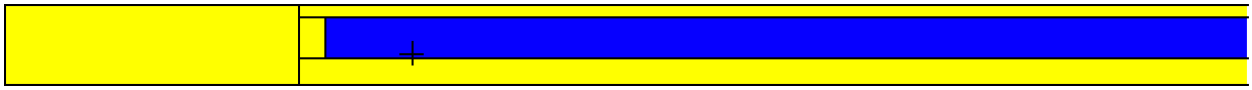

Figure 14: Cut MCNP model of the TEX-Cl 3/16" NaCl absorber with encapsulation, as an example. Only the edge of the plate is shown.

3.2 Design Process

In the TEX-Cl CED-2 for IER-499 [11] the design process utilized Bayesian Optimization (BO) [8] techniques and parametric studies to obtain critical TEX configurations with variable polyethylene and NaCl absorber thicknesses. Constraint parameters of the BO were the thermal capture sensitivity, an overall height to diameter ratio less than 1.5, and a k_{eff} less than 0.9 for half of the stack (to ensure the experiment can be safely executed). The models were also constrained with the existing HEU plate inventory and geometries. The BO search was focused on finding configurations with maximum similarity with the sensitivity profiles from the Y-12 electrorefining system, as modeled in the NCS design evaluation. BO optimization was run with 100 iterations with the polyethylene thickness range set to 0"-2.5" and the NaCl absorber thickness range set to 0"-1". Figure 15 shows the result of the BO for the 6-layer standard configurations, showing the thermal sensitivity with respect to the polyethylene and absorber thicknesses and the constraint function (k_{eff}) which shows a critical "valley" (white line) in which a configuration is critical. The BO produced numerous critical configurations, but the configurations were further tuned to match producible dimensions, such that polyethylene and absorber thicknesses were in 1/16" increments. The similarity was assessed by two main characteristics of the sensitivity profiles. The first being a high thermal capture sensitivity of ^{35}Cl and the second being a sensitivity profile shape similar

to the electro-refiner calculations. The BO results served as a basis for additional configurations with more dense absorber material.

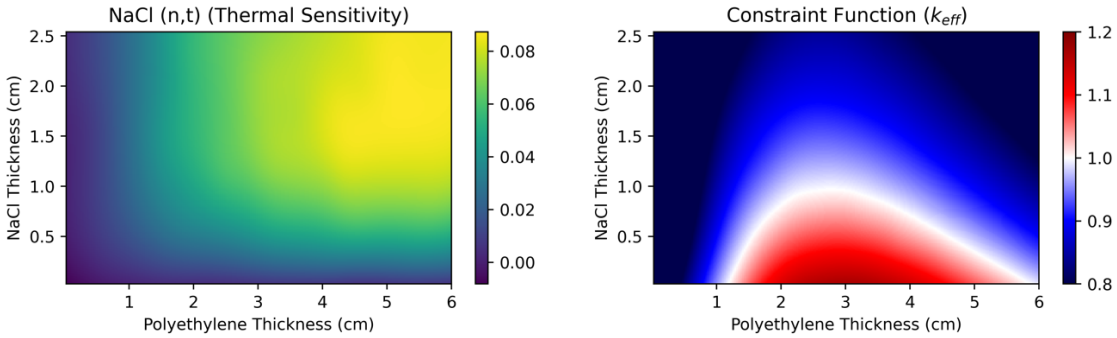

Figure 15: An example of the Bayesian Optimization results for the 6-layer standard configuration.

The energy groups for calculating the thermal capture sensitivities were first set to the three-energy group structure: thermal (0 MeV – 0.625E-6 MeV), intermediate (0.625E-6 MeV-0.1 MeV), and fast energy groups (0.1 MeV – 20 MeV). To quantitatively compare the sensitivity profiles of the tuned critical configuration to the application cases the G parameter was used [21], the same metric selected in the TEX-Cl CED-2. In brief, the G parameter is defined as

$$G = 1 - \frac{\mathbf{S_1}^T \mathbf{S_2}}{0.5(|\mathbf{S_1}|^2 + |\mathbf{S_2}|^2)}, \quad (1)$$

where it compares the similarity between sensitivity profiles $\boldsymbol{S}_1$ and $\boldsymbol{S}_2$. The maximal similarity occurs as G approaches 0, meaning that a smaller G value refers to the most similar sensitivity profiles.

3.3 TEX-Designs

This section outlines the parameters of the selected models. In addressing the needs of the INL application cases and the TerraPower needs for MCRE and MCFR. Three configurations were selected to be performed experimentally. One of the configurations primarily addresses the nuclear data needs of the ^{35}Cl(n,p) cross section. Appendix D shows the stacking configuration for all the identified configurations.

3.3.1 Configuration Overview

3.3.1.1 Polyethylene Reflected Configurations

Table 13 and Table 14 display the physical and neutronics parameters for the two polyethylene reflected configuration models, respectively. The 3/8”-moderator model was selected for achieving a good mixture of thermal and fast sensitivity. The 1”-moderator model was selected for achieving the lowest G parameter compared to the INL cases as well as maximum thermal sensitivity. The maximum thermal and fast capture sensitivities are shown for all models. The

lowest G parameter calculated with the INL/TerraPower application cases is shown for each model.

Table 13: Physical characteristics for the selected standard stacking configurations.

Number of Layers	HDPE Moderator Thickness (in)	NaCl Absorber Thickness (in)	HEU Mass (g)	HDPE Top Reflector Thickness (in)	H/D Ratio
14	3/8”	1/2”	87,496	1”	1.04
12	1”	1/2”	57,422	3/4”	1.34

Table 14: Neutronics characteristics for the selected standard stacking configurations. Statistical uncertainty in k_{eff} for both models is at 0.00007.

Number of Layers	k_{eff}	k_{eff} of Half Stack	Maximum Thermal Capture Sensitivity Amplitude	Maximum Fast Capture Sensitivity Amplitude	Minimum G Parameter for INL	Thermal Fission Fraction (%)	Intermediate Fission Fraction (%)	Fast Fission Fraction (%)
14	1.00138	0.85095	0.0171	0.0036	0.192	30.19	49.38	20.43
12	1.00400	0.86832	0.0419	0.0023	0.035	51.23	34.95	13.81

The sensitivity profiles are compared to the Idaho National Laboratory / TerraPower application case sensitivity profiles in, introduced in Section 1, shown in Figure 16 and Figure 17. Included in the sensitivity profile plots are the corresponding residuals which are simply the deviation of the application case profiles to that of the proposed configuration. The comparison of the total capture sensitivity to the sensitivity profiles of INL/TerraPower shows that partial similarities exist (i.e. good similarity in the thermal or the fast energy region) providing validation for their needs. Figure 18 and Figure 19 show the fission fractions per unit lethargy for the two configurations.

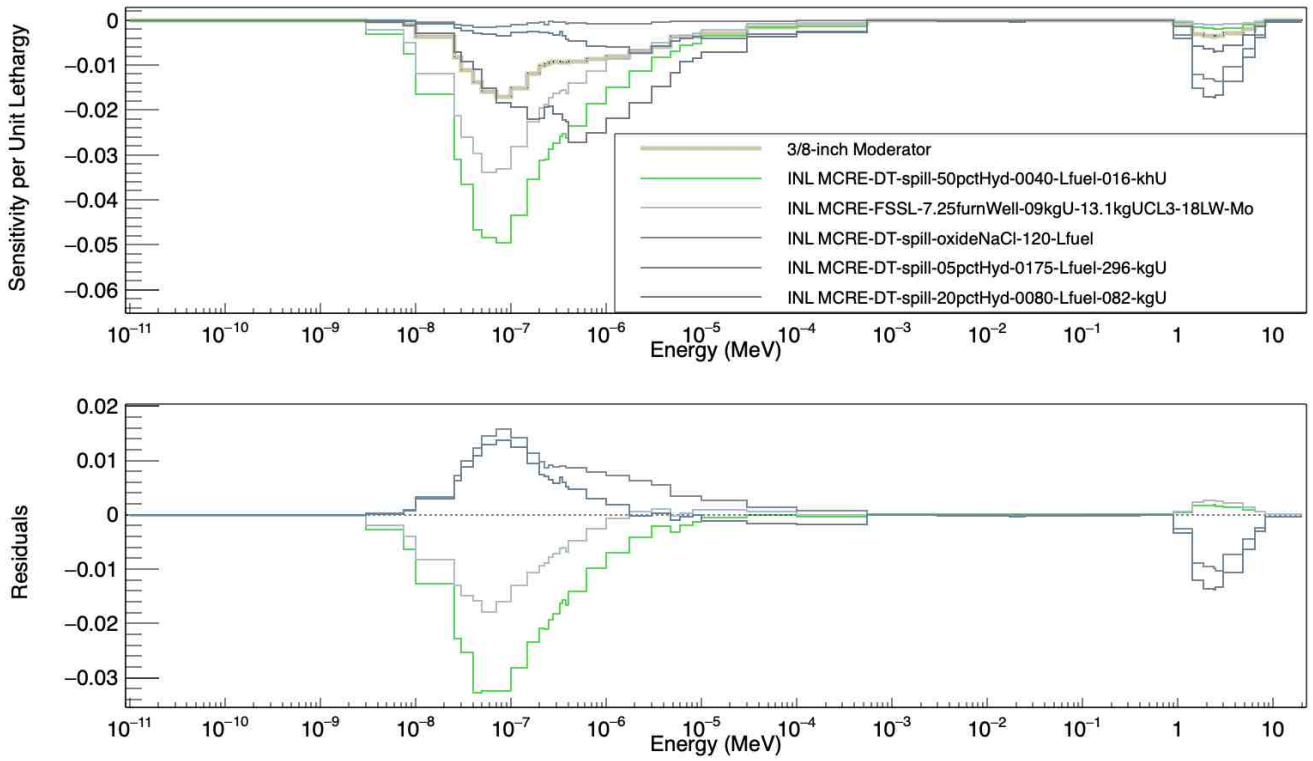

Figure 16: Neutron capture sensitivity profile for the 3/8”-moderator configuration compared to the INL application case sensitivity profiles.

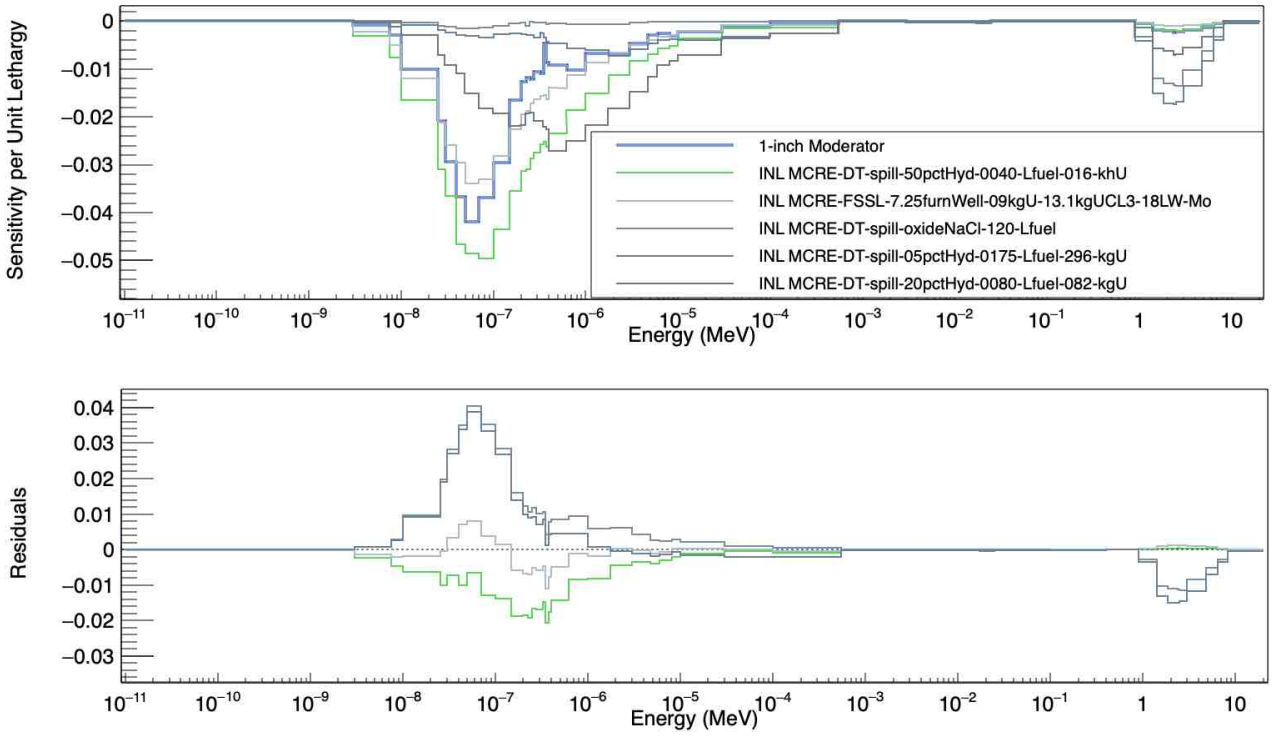

Figure 17: Neutron capture sensitivity profile for the 1”-moderator configuration compared to the INL application case sensitivity profiles.

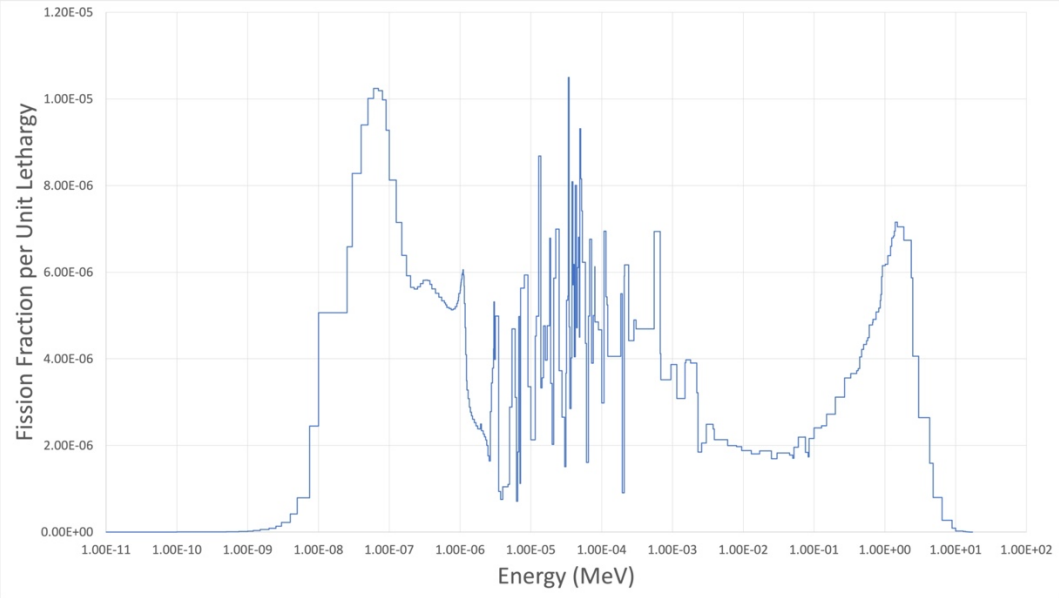

Figure 18: Fission fraction per unit lethargy for the 3/8”-moderator configuration.

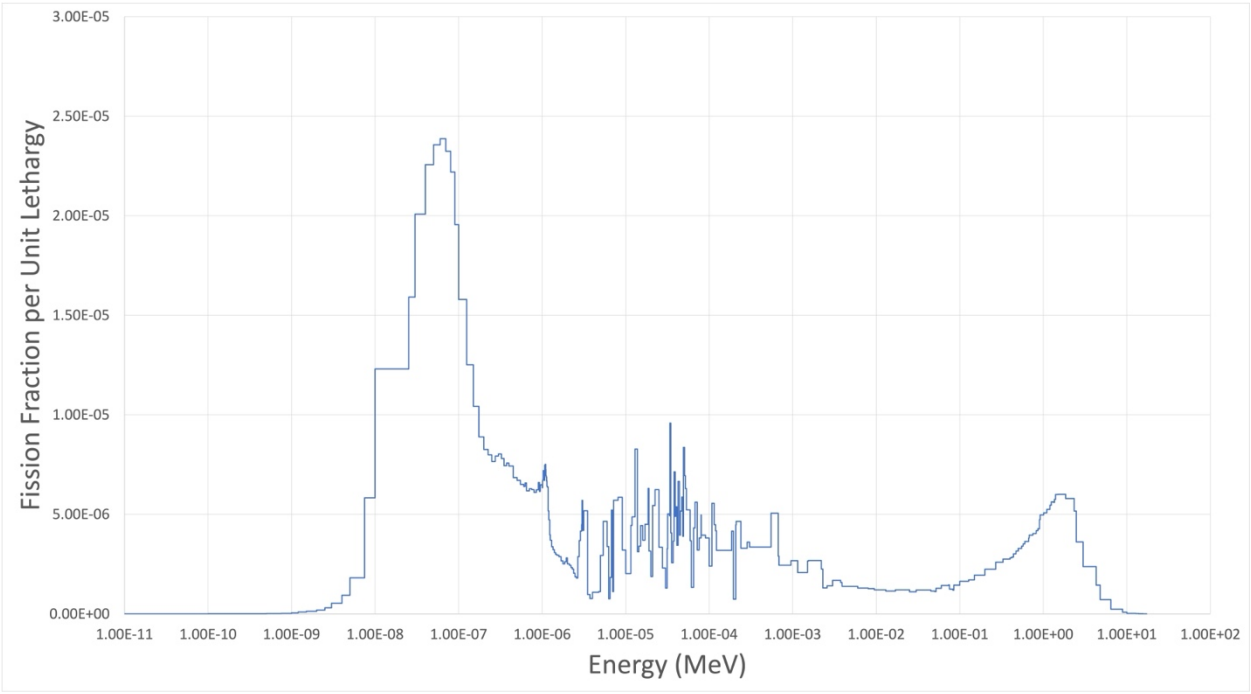

Figure 19: Fission fraction per unit lethargy for the 1”-moderator configuration.

3.3.1.2 Copper Reflected Configurations

Two copper reflected configurations were identified: one that uses a central alignment tube and one that utilizes a copper reflector sleeve around the 15” HEU plates to perform alignment. This is to account for possible manufacturing challenges, which allows us to select either if the manufacturing process becomes more advantageous than the other. The central alignment tube configuration is presented here as the Zeus-like configuration. The copper sleeve, which is less preferable from an operational standpoint, will be presented in Appendix D.

Table 13 and Table 14 display the physical and neutronics parameters for the Zeus-like copper reflected configuration model, respectively. This configuration is predicted to have 18 fuel layers.

Table 15: Physical characteristics for the selected standard stacking configurations.

Number of Layers	HDPE Moderator Thickness (in)	NaCl Absorber Thickness (in)	HEU Mass (g)	H/D Ratio
18 - Tube	-	1”	219,479	1.50

Table 16: Neutronics characteristics for the selected standard stacking configurations. Statistical uncertainty in k_{eff} for both models is at 0.00007.

Number of Layers	k_{eff}	k_{eff} of Half Stack	Maximum Thermal Capture Sensitivity Amplitude	Maximum Fast Capture Sensitivity Amplitude	Minimum G Parameter for INL	Thermal Fission Fraction (%)	Intermediate Fission Fraction (%)	Fast Fission Fraction (%)
18 - Tube	1.00031	0.72830	-	0.0086	0.12	0.00	33.26	66.74

The sensitivity profiles are compared to the Idaho National Laboratory / TerraPower application case sensitivity profiles in, introduced in Section 1, shown in Figure 20. Included in the sensitivity profile plot is the corresponding residuals which are simply the deviation of the application case profiles to that of the proposed configuration. This configuration is predominantly fast, providing sensitivity to the fast bump in the INL/TerraPower profiles as well as validation for the $^{35}Cl(n,p)$ cross section. Figure 21 shows the fission fractions per unit lethargy for the configuration.

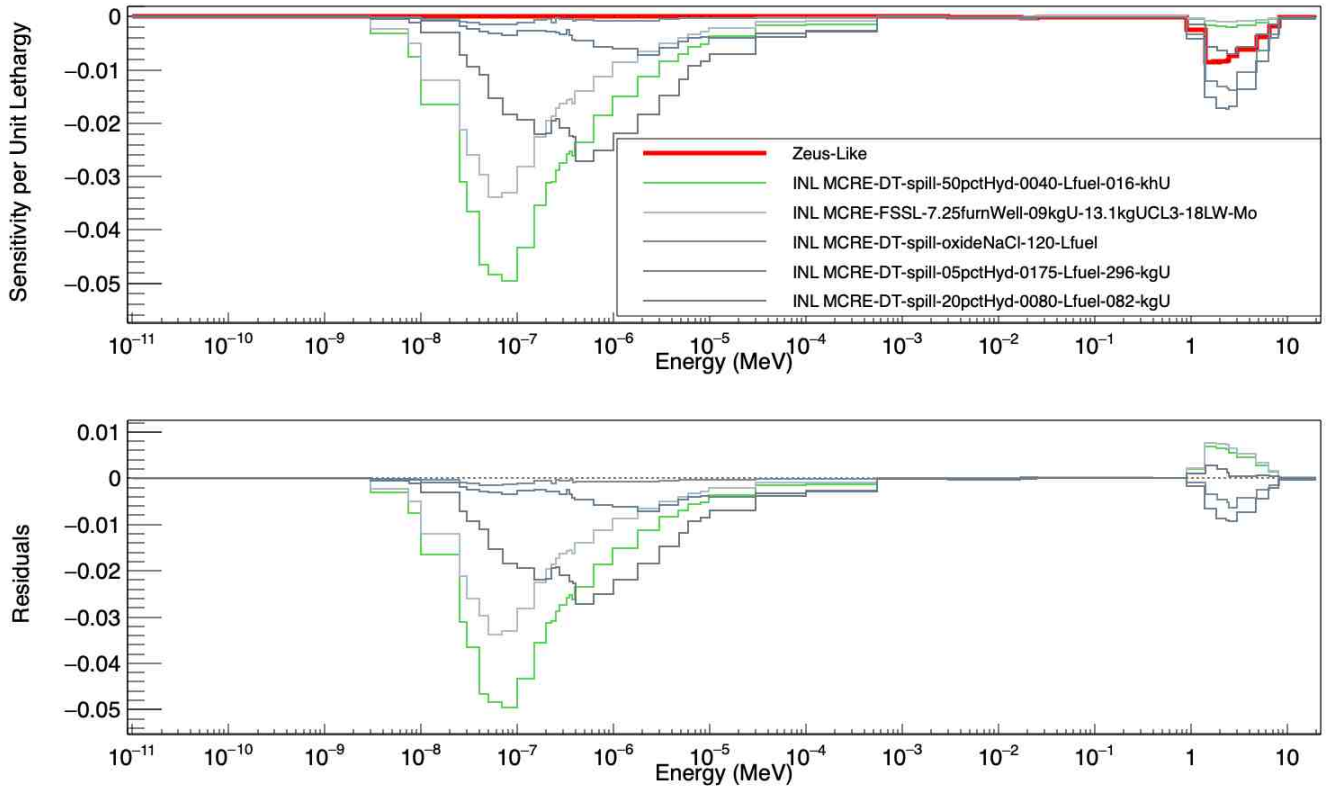

Figure 20: Neutron capture sensitivity profile for the Zeus-like configuration with the inner alignment tube compared to the INL application case sensitivity profiles.

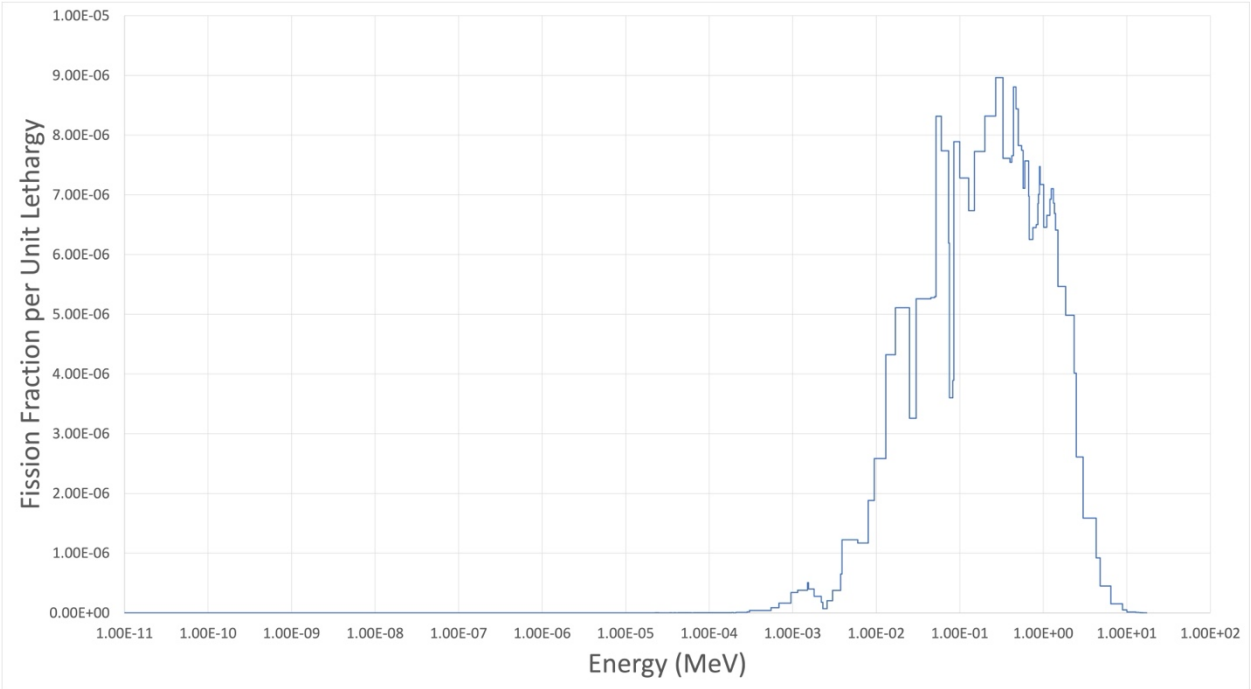

Figure 21: Fission fraction per unit lethargy for the Zeus-like configuration with the inner alignment tube.

3.4 Uncertainty and Bias Characterization

The effects on the effective neutron multiplication factor of various uncertainties in the experimental data are presented in this section. For absorber specific uncertainties, the uncertainty quantification was estimated based on existing uncertainty calculations for the previous TEX-Cl experiment. Other, more general, uncertainties were taken directly from the original CED-2 and are expected to be representative of the new configurations. These uncertainties were generally derived or pulled from IER-297-CED-2 [12]. Copper reflector-based uncertainties were estimated via previous benchmark calculations in [7]. The bias inherent in the simulations due to exclusion of certain model parameters is also evaluated in Section 3.4.2.

3.4.1 Uncertainty Characterization

3.4.1.1 NaCl Absorber Thickness

The thickness of the NaCl absorber plate was perturbed by 0.02 cm (roughly 4%) in the benchmark model while keeping the mass constant. The bottom of the encapsulation was perturbed by the same amount in the opposite direction in order to maintain the same overall absorber assembly thickness. An increase in overall absorber thickness resulted in a -0.00179 change in k_{eff} and a decrease in absorber thickness resulted in a +0.00191 change in k_{eff}. Both configurations were run to a 0.00004 statistical uncertainty.

3.4.1.2 NaCl Absorber Mass

The mass of NaCl absorber plate was increased and decreased by 10 grams (~1.5%) in the model while keeping the volume constant. A +/- 1.5% uncertainty in the mass is encompassing of the empirical uncertainty on the density. Uncertainty related to the NaCl mass will be reduced by precisely weighing the plates in the experiments. An increase in mass resulted in a -0.00093 change in k_{eff} where a decrease by mass resulted in a + 0.00083 difference. Both calculations were run to a 0.00004 statistical uncertainty.

3.4.1.3 NaCl Absorber H_2O Content

The water (moisture) content of the NaCl was found to be at maximum 160 ppm. The final configurations assume pure NaCl without the introduction of water. Detailed models for the original TEX-Cl indicate that the introduction of this limited quantity of moisture has a negligible effect on the resulting k_{eff}.

3.4.1.4 Copper Reflector Mass

The mass of the reflector pieces was perturbed by varying amounts, according to the part mass, while retaining a constant volume. These calculations were run to a precision of 0.00002. Each part type sensitivity was added linearly, and each component was added in quadrature to obtain the resulting effect on k_{eff}, which was found to be 0.00062 [7].

3.4.1.5 Copper Reflector Dimensions

The dimensions of the reflector pieces were perturbed by varying amounts, according to the part dimensions, while retaining a constant mass. These calculations were run to a precision of 0.00002. The resulting effect on keff was found to be 0.00004 [7].

3.4.1.6 Copper Reflector Composition

The composition (impurities) of the reflector pieces were perturbed with copper being the balance. The uncertainties were assessed to be correlated; therefore, the uncertainties were added linearly. These calculations were run to a precision of 0.00002. The resulting effect on k_{eff} was found to be 0.00004 [7].

3.4.1.7 Copper Reflector Stack Gaps

Gaps in the side reflectors were perturbed by 0.006 in, which increased or decreased gaps in the reflector stack. These calculations were run to a precision of 0.00002. The resulting effect on k_{eff} was found to be 0.00020 [7].

3.4.1.8 Uranium Plate Mass

The Jemima plates mass information for the calculations described in this report were taken from the ICSBEP benchmark HEU-MET-INTER-006 [12]. The following description of the mass uncertainties is excerpted from this report and no additional measurements have been made for the proposed experiments.

The absolute uncertainty (standard deviation) for the total mass of a sum of N masses is,

$$\sigma_T = \sqrt{N^2{\sigma_r}^2 + N^2{\sigma_s}^2 + \frac{N^2{\sigma_c}^2}{12}}$$

where σ_T = absolute uncertainty in the total mass,

σ_r = absolute random measurement error,

σ_s = absolute systemic measurement error,

σ_c = round-off resolution, and

N = total number of pieces of the mass, each of which is measured.

The factor of 12 appears because the density function for the round-off resolution is assumed to be uniform over the interval from 0 to σ_c.

The HEU masses were calculated at LANL by subtracting the tare mass from the gross mass. The variance of the net mass (i.e., the mass of the HEU disk or ring) is the sum of the variances of the two measured masses. In this instance, the variances of the gross and tare masses are the same. Therefore, the variance of the net mass is twice the variance of the individual mass, and the standard deviation is the square root of two times the result given by the equation above.

Four “Calibration Certificates” for the balance used to weigh the HEU and graphite plates were examined. Before adjustment, the balances were found to measure to an accuracy ranging from ±0.2 g to ±1.3 g. After adjustment, the range was from ±0.0 g to ±0.2 g.

Based on the above information, it is conservatively assumed that both the random and systematic absolute uncertainties for the balance are ±1.3 g. The round-off resolutions for the HEU disks are taken to be 1 g.

The resulting standard deviation in the mass of the Jemima plates is reported to be ±0.03%. These values were used for uncertainty analysis in this report.

3.4.1.9 Polyethylene Moderator Plate Mass

The density of polyethylene plates used in the benchmark model is 0.967 g/cm^3. Densities of the polyethylene plates to be used in the experiments are not yet known. The density of polyethylene was increased by 0.005 g/cm^3 (a change of 0.517%, slightly more than double that used by HEU-MET-THERM-001 [13] and considered to be a bounding value on the uncertainty in the mass), and the change in k_{eff} was 0.00086. Uncertainty related to polyethylene moderator mass will be reduced by precisely weighing all new parts.

3.4.1.10 Polyethylene Reflector Mass

The density of polyethylene reflector surrounding the Jemima fuel plates used in the benchmark model is 0.967 g/cm^3. The density of HDPE was increased by 0.005g/cm^3 (a change of 0.517%, slightly more than double that used by HEU-MET-THERM-001 and considered to be a bounding value on the uncertainty in the mass), and the change in k_{eff} was 0.00040.

3.4.1.11 ^{235}U Enrichment

The U-235 enrichment values shown in Table 1 were taken from several benchmark reports that used the Jemima plates [15-17] and the standard deviation was calculated to be 0.110419%. The U-235 enrichment for each plate was increased by 0.110419 wt% with an equivalent decrease in the concentration of U-238 while all other isotopes and impurities were left unchanged. The resulting change in k_{eff} was 0.00042.

3.4.1.12 Room Return

Bias inherent to the calculations due to modeling the experimental configurations in a vacuum and excluding the effects of room return was examined by modeling the room in which the experiments will take place and calculating the resulting change in k_{eff}. The configuration was located with the bottom of the assembly 4 feet above the floor and the central axis of the assembly 6 feet from the nearest wall. The simulations excluding room return underestimate k_{eff} by 0.00064.

3.4.1.13 Uranium Plate Impurities

Some impurities in the Jemima plates are undetectable when they are present in quantities below a certain detection threshold. In these cases, they are reported as "<XX" in Table 3 and were omitted from the model. The effect of this uncertainty in HEU impurities was calculated by including these impurities at the minimum detectable limit, or the highest value measured for a single plate, whichever was higher, as shown in Table 17. The uncertainty in k_{eff} associated with minimum detectable impurity content was calculated as 0.00004.

Table 17: HEU Impurity Content Added for Uncertainty Analysis.

Impurity	Content (ppm)
Li	0.1
Be	0.1
Na	1.0
Mg	1.0
Ca	2.0
V	20.0
Co	5.0
Sn	1.0
Pb	5.0

All simulations presented in this work include measured impurities in the Jemima plates, but it may be desirable to simplify the model by removing them in the future. For this reason, and to account for any errors in the measurement of these impurities, the bias associated with excluding impurities in the fuel was estimated by simulating the conservative case of zero impurities. The model excluding impurities overestimated k_{eff} by 0.00019.

3.4.2 Uncertainty and Bias Summary

Table 18 outlines the overall source of uncertainties for the proposed configurations. These are assumed to be the same for all models. Table 19 shows the resulting uncertainties for the NaCl absorbers. In Table 20, the biases presented in both of removing HEU impurities and including room return were directly taken from IER-297-CED2. These were considered appropriate for this stage of the design.

Table 18: Summary of uncertainties for non-absorber calculations. Standard deviation calculated by MCNP6 in all models was 0.00002.

Source of Uncertainty	Parameter Variation	Calculated Effect, Δk_{eff}
HEU Plate Mass	+0.03%	0.00016
HEU Plate Mass	-0.03%	-0.00006
HDPE Moderator Mass	+0.005 g/cm^3	0.00086
HDPE Reflector Mass	+0.005 g/cm^3	0.00040
HEU Plate Gaps	0.00127 cm	-0.00044
U-235 Enrichment	+0.110419%	0.00042
HEU Impurities	"<XX" Impurities Added	0.00004

Source of Uncertainty	Parameter Variation	Calculated Effect, Δk_{eff}
Assembly Alignment	1/8th Inch Offset Added	-0.00006
Cu Reflector Mass	Various	0.00062
Cu Reflector Dimensions	Various	0.00004
Cu Reflector Composition	Various	0.00004
Cu Side Reflector Gaps	+/-0.006 in.	0.00020
Quadrature Sum		**0.00132**

Table 19: Summary of uncertainties for NaCl Absorber calculations. Standard deviation calculated by MCNP6 in all models was 0.00007.

Source of Uncertainty	Parameter Value Used	Parameter Variation	Calculated $\Delta k_{eff+} - \Delta k_{eff-}$	Standard Uncertainty in Δk_{eff}
NaCl Plate Thickness	0.635 cm	+/- 1%	-0.00370	0.00021
NaCl Plate Mass	671.83 g	-/+ 1.5%	-0.00176	0.00036
H_2O Content in NaCl Plate	0% H_2O content	-	-	Negligible
			Quadrature Sum	**0.00042**

Table 20: Summary of bias sources for excluding parameters.

Source of Bias	Parameter Variation	Δk_{eff}	Standard Deviation Calculated by MCNP6
HEU Impurities	Removed	0.00019	0.00002
Room Return	Added	0.00064	0.00002

3.5 Reactivity analysis

Two main methods for reactivity control explored in this design report are the total HEU mass and the upper reflector thickness. Each of the proposed configurations were specifically designed so that the total HEU mass could be increased and decreased. Similarly, they were also designed to allow for the addition or subtraction of upper reflector thickness.

3.5.1 Upper Reflector Thickness

Fine reactivity control for the polyethylene reflected configurations is primarily performed by varying the upper reflector thickness. As such, calculations for those two configurations were performed to show the effect that decreasing and increasing the upper reflector thickness in 1/8" or 1/16" increments would have on k_{eff}. Figure 22 shows the reactivity as a function of upper reflector thickness for the two polyethylene reflected configurations. Table 21 tabulates the same data, showing the difference in k_{eff} per upper reflector thickness step as well as that difference in terms of cents of reactivity. The reactivity worth in cents is estimated with the β_{eff} value estimated in the simulation (0.00744 and 0.00756 for the 1"-moderator and 3/8"-moderator configuration, respectively).

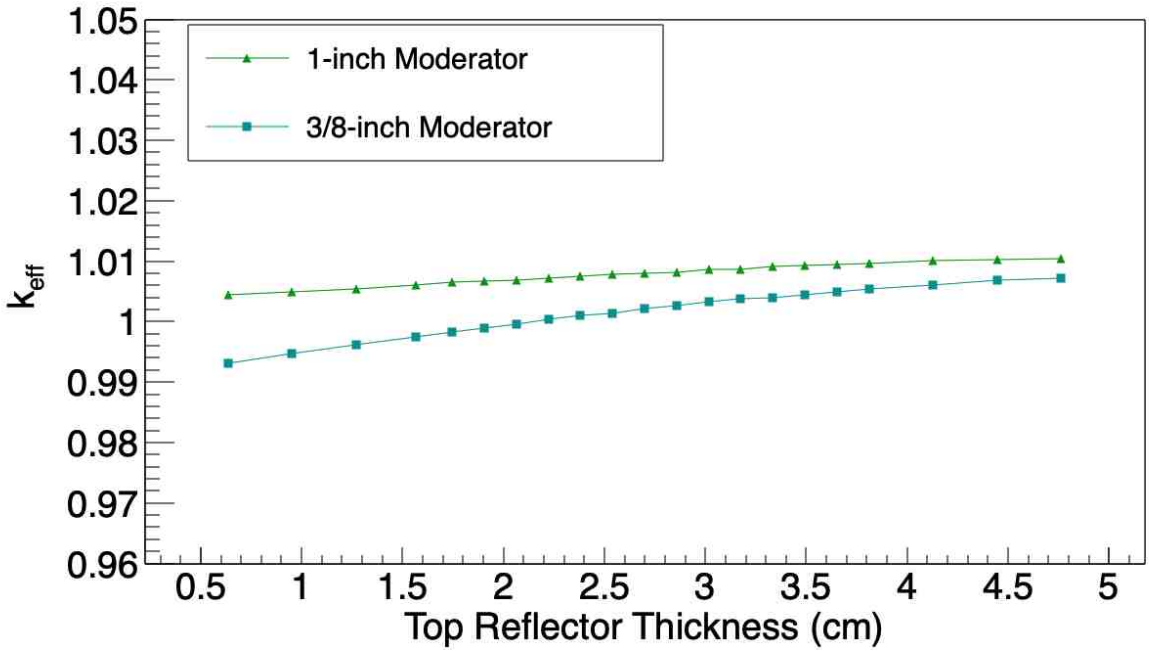

Figure 22: k_{eff} as a function of total top reflection (cm) for the polyethylene reflected configurations.

Table 21: Δk_{eff} as a function of total upper reflector thickness (inch) for the polyethylene reflected configurations.

Upper Reflector Thickness (cm)	Upper Reflector Thickness (in)	1"-Moderator			3/8"-Moderator		
		keff	δkeff	δkeff (¢)	keff	δkeff	δkeff (¢)
0.635	0.250	1.00173	-	-	0.99316	-	-
0.953	0.375	1.00217	0.00044	5.91	0.99469	0.00153	20.24
1.270	0.500	1.00266	0.00049	6.59	0.99611	0.00142	18.78
1.568	0.617	1.00336	0.0007	9.41	0.99755	0.00144	19.05
1.746	0.688	1.0038	0.00044	5.91	0.99823	0.00068	8.99
1.905	0.750	1.004	0.0002	2.69	0.99896	0.00073	9.66
2.064	0.813	1.00414	0.00014	1.88	0.99952	0.00056	7.41
2.223	0.875	1.00456	0.00042	5.65	1.00035	0.00083	10.98
2.381	0.938	1.00487	0.00031	4.17	1.00096	0.00061	8.07
2.540	1.000	1.00513	0.00026	3.49	1.00138	0.00042	5.56
2.699	1.063	1.00528	0.00015	2.02	1.00211	0.00073	9.66
2.858	1.125	1.00552	0.00024	3.23	1.00263	0.00052	6.88
3.016	1.188	1.00601	0.00049	6.59	1.00326	0.00063	8.33
3.175	1.250	1.00605	0.00004	0.54	1.00371	0.00045	5.95
3.334	1.313	1.00643	0.00038	5.11	1.00401	0.0003	3.97
3.493	1.375	1.00659	0.00016	2.15	1.00446	0.00045	5.95
3.651	1.438	1.00671	0.00012	1.61	1.00499	0.00053	7.01
3.810	1.500	1.00696	0.00025	3.36	1.00538	0.00039	5.16
4.128	1.625	1.00736	0.0004	5.38	1.00606	0.00068	8.99
4.445	1.750	1.00767	0.00031	4.17	1.0068	0.00074	9.79
4.763	1.875	1.00783	0.00016	2.15	1.00721	0.00041	5.42
5.080	2.000	1.00818	0.00035	4.70	1.00766	0.00045	5.95

3.5.2 Aluminum Spacer Thickness

Unlike the polyethylene reflected configurations, the copper reflected configurations do not have the option of fine reactivity control via upper reflector thickness. Instead, we will rely on interstitial aluminum which may be inserted into the assembly to decrease the reactivity and HEU plate swaps to alter the fuel mass which will tune the reactivity of the system. For these calculations, the aluminum spacers are placed on top of the upper most aluminum absorber encapsulation of the lower stack. Essentially, this acts just like separation, presented in Section 3.5.4, but with aluminum filling the gap. Aluminum thickness steps of 1/8" and 1/16" were used up to 2" of total aluminum thickness. Figure 23 shows the reactivity as a function of interstitial aluminum thickness for the copper reflected configuration. Table 22 tabulates the same data, showing the difference in

k_{eff} per aluminum thickness step as well as that difference in terms of cents of reactivity. The reactivity worth in cents is estimated with the β_{eff} value estimated in the simulation (0.00720 for this configuration).

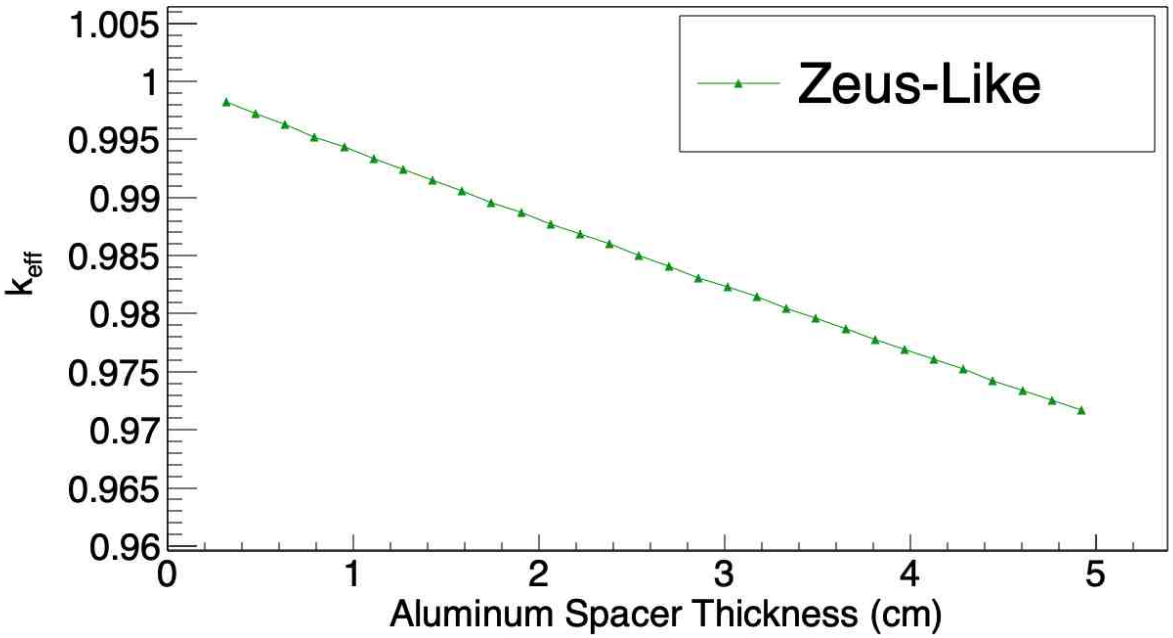

Figure 23: keff as a function of aluminum spacer thickness (cm) for the copper reflected configurations.

Table 22: Δk_{eff} as a function of interstitial aluminum thickness (cm) for the copper reflected configurations.

Al Spacer Thickness (cm)	Al Spacer Thickness (in)	Zeus-Like		
		keff	keff	keff (¢)
0.318	0.125	0.99824	-	-
0.476	0.188	0.99724	-0.00100	-13.44
0.635	0.250	0.99627	-0.00097	-13.04
0.794	0.313	0.99522	-0.00105	-14.11
0.953	0.375	0.99437	-0.00085	-11.42
1.111	0.438	0.99336	-0.00101	-13.58
1.270	0.500	0.99243	-0.00093	-12.50
1.429	0.563	0.99152	-0.00091	-12.23
1.588	0.625	0.99061	-0.00091	-12.23
1.746	0.688	0.98955	-0.00106	-14.25
1.905	0.750	0.98868	-0.00087	-11.69
2.064	0.813	0.98772	-0.00096	-12.90
2.223	0.875	0.98683	-0.00089	-11.96
2.381	0.938	0.98600	-0.00083	-11.16
2.540	1.000	0.98497	-0.00103	-13.84
2.699	1.063	0.98408	-0.00089	-11.96
2.858	1.125	0.98308	-0.00100	-13.44
3.016	1.188	0.98232	-0.00076	-10.22
3.175	1.250	0.98148	-0.00084	-11.29
3.334	1.313	0.98045	-0.00103	-13.84
3.493	1.375	0.97959	-0.00086	-11.56
3.651	1.438	0.97869	-0.00090	-12.10
3.810	1.500	0.97778	-0.00091	-12.23
3.969	1.563	0.97694	-0.00084	-11.29
4.128	1.625	0.97609	-0.00085	-11.42
4.286	1.688	0.97520	-0.00089	-11.96
4.445	1.750	0.97421	-0.00099	-13.31
4.604	1.813	0.97336	-0.00085	-11.42
4.763	1.875	0.97255	-0.00081	-10.89
4.921	1.938	0.97170	-0.00085	-11.42
5.080	2.000	0.97087	-0.00083	-11.16

3.5.3 HEU Plates Swaps

This section outlines the effect that changing the fissile material mass has on the reactivity of the system. The HEU plates that will be used in the experiments each have a specific hole diameter and total amount of fissile material. The original configurations can be found in Appendix C and the detailed plate swap tables can be found in Appendix B. The reactivity as a function of mass for all of the proposed configurations are shown in Figure 24 through Figure 26 and tabulated in Table 23 through Table 25.

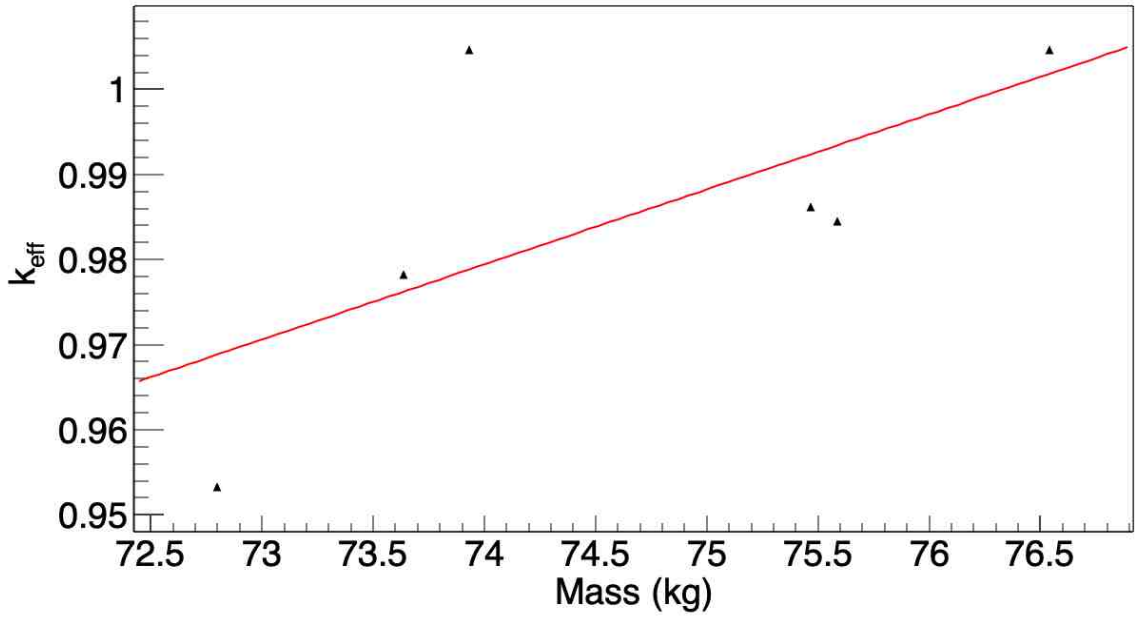

Figure 24: Reactivity as a function of HEU mass for the 1" Moderator Configuration. The upper reflector thickness in all the models was kept at 1". Δk_{eff} per kg is equal to 0.0088.

Table 23: k_{eff} as a function of total HEU mass for the 1" Moderator Configuration.

Alt Num	Mass (kg)	keff
1	75.585	0.98447
2	72.798	0.95330
3	73.635	0.97824
4	75.467	0.98621
5	73.93	1.00462
Original	76.541	1.00460

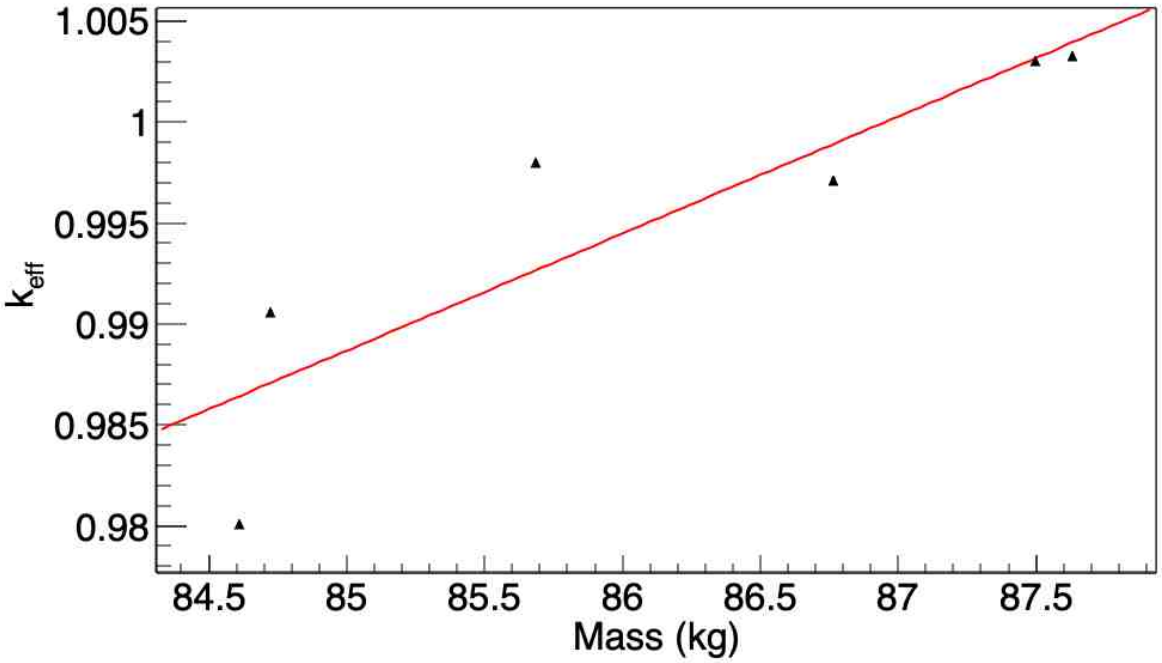

Figure 25: Reactivity as a function of HEU mass for the 3/8" Moderator Configuration. The upper reflector thickness in all the models was kept at 1". Δk_{eff} per kg is equal to 0.0058.

Table 24: k_{eff} as a function of total HEU mass for the 1" Moderator Configuration.

Alt Num	Mass (kg)	keff
1	85.685	0.99801
2	84.721	0.99059
3	87.631	1.00328
4	84.611	0.98009
5	86.763	0.99714
Original	87.496	1.00304

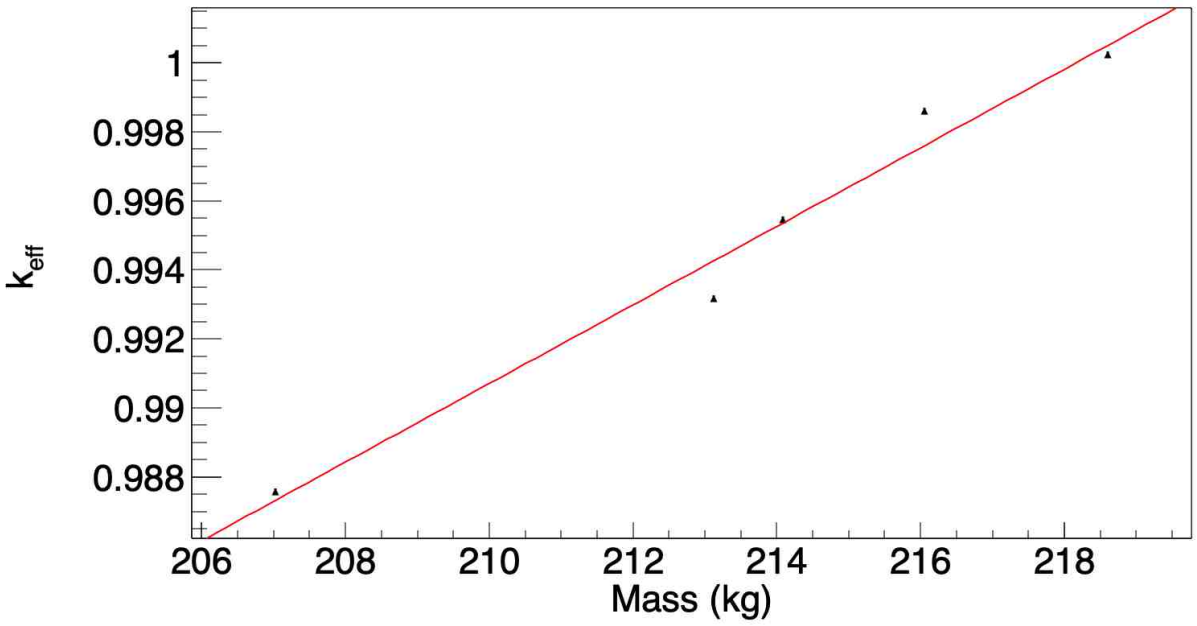

Figure 26: Reactivity as a function of HEU mass for the Zeus-Like Configuration. Δk_{eff} per kg is equal to 0.0011.

Table 25: k_{eff} as a function of total HEU mass for the Zeus-Like Configuration.

Alt Num	Mass (kg)	keff
1	214.09	0.99545
2	218.61	1.00024
3	213.12	0.99317
4	216.05	0.99860
5	207.02	0.98757
Original	216.87	1.00026

3.5.4 Separation Study

For each of the planned configurations the bottom half of the assembly is lifted upwards to meet the upper half and achieve criticality. In the MCNP6 models, the lower portion of the TEX geometry was translated away from the center as seen in Figure 27. For the polyethylene reflected configurations, the entire lower core stack and annular reflectors were translated down. For the copper reflected configurations, only the lower core stack was translated down. Investigating the effect of separation on criticality allows the operator to stay in control of the reactivity as the two halves close. This study was performed at the separation distances of 63.5 cm, 38.1 cm, 25.4 cm,

12.7 cm, 10.16 cm, 7.62 cm, 6.35 cm, 5.08 cm, 4.445 cm, 3.81 cm, 3.175 cm, 2.54 cm, 2.2225 cm, 1.905 cm, 1.5875 cm, 1.27 cm, 0.9525 cm, 0.79375 cm, 0.635 cm, 0.47625 cm, 0.3175 cm, 0.15875 cm. Note that the separation distance of 63.5 cm (25”) is taken as the handstack k_{eff} as it is assumes maximal separation. It should be noted that even at 12.7 cm (5”) of separation the handstack limit is satisfied. Table 26 tabulates the reactivity as a function of separation distance for the standard configurations while Figure 28 shows the reactivity curve graphically for all of the configurations. Table 26 tabulates the reactivity as a function of separation distance for the sandwich configurations.

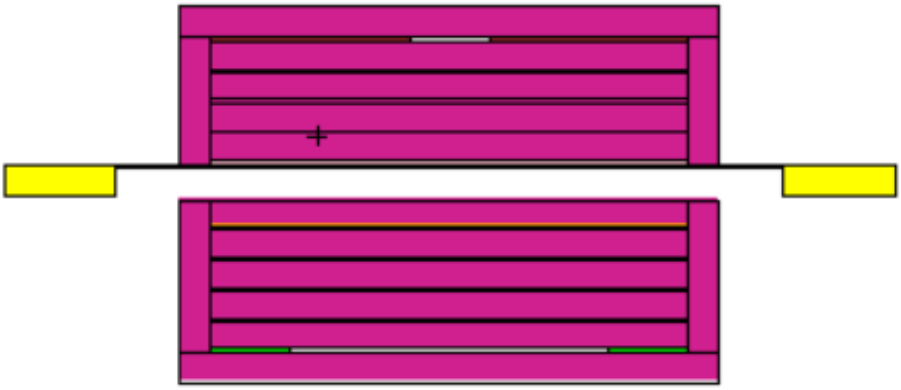

Figure 27: The separation of the TEX body at the platen. As the bottom half of the assembly moves on the lift, the separation changes.

Table 26: Reactivity as a function of separation distance starting at 25" (63.5 cm) to close (0" cm) separation for the standard configurations. Statistical uncertainty in k_{eff} for all models is at 0.00007. Reactivity in cents is based on the calculated β_{eff} from the final configurations.

Separation Distance (in)	3/8"-Moderator			1"-Moderator			Zeus-Like		
	keff	keff	keff (¢)	keff	keff	keff (¢)	keff	keff	keff (¢)
25	0.85095	-	-	0.86832	-	-	0.72830	-	-
15	0.85379	0.00284	39.01	0.87146	0.00314	44.54	0.77301	0.04471	620.97
10	0.85940	0.00561	77.06	0.87691	0.00545	77.3	0.83311	0.06010	834.72
5	0.88006	0.02066	283.79	0.89463	0.01772	251.35	0.91345	0.08034	1115.83
4	0.88994	0.00988	135.71	0.90229	0.00766	108.65	0.92869	0.01524	211.67
3	0.90367	0.01373	188.6	0.91319	0.01090	154.61	0.94443	0.01574	218.61
2.5	0.91297	0.00930	127.75	0.92044	0.00725	102.84	0.95245	0.00802	111.39
2	0.92415	0.01118	153.57	0.92950	0.00906	128.51	0.96102	0.00857	119.03
1.75	0.93064	0.00649	89.15	0.93475	0.00525	74.47	0.96555	0.00453	62.92
1.5	0.93783	0.00719	98.76	0.94082	0.00607	86.1	0.96987	0.00432	60.00
1.25	0.94593	0.00810	111.26	0.94773	0.00691	98.01	0.97459	0.00472	65.56
1	0.95497	0.00904	124.18	0.95557	0.00784	111.21	0.97926	0.00467	64.86
0.875	0.95957	0.00460	63.19	0.95998	0.00441	62.55	0.98169	0.00243	33.75
0.75	0.96480	0.00523	71.84	0.96463	0.00465	65.96	0.98430	0.00261	36.25
0.625	0.97019	0.00539	74.04	0.96968	0.00505	71.63	0.98682	0.00252	35.00
0.5	0.97570	0.00551	75.69	0.97512	0.00544	77.16	0.98946	0.00264	36.67
0.375	0.98136	0.00566	77.75	0.98079	0.00567	80.43	0.99216	0.00270	37.50
0.3125	0.98469	0.00333	45.74	0.98388	0.00309	43.83	0.99351	0.00135	18.75
0.25	0.98756	0.00287	39.42	0.98700	0.00312	44.26	0.99479	0.00128	17.78
0.1875	0.99061	0.00305	41.9	0.99030	0.00330	46.81	0.99624	0.00145	20.14
0.125	0.99364	0.00303	41.62	0.99357	0.00327	46.38	0.99751	0.00127	17.64
0.0625	0.99667	0.00303	41.62	0.99678	0.00321	45.53	0.99890	0.00139	19.31

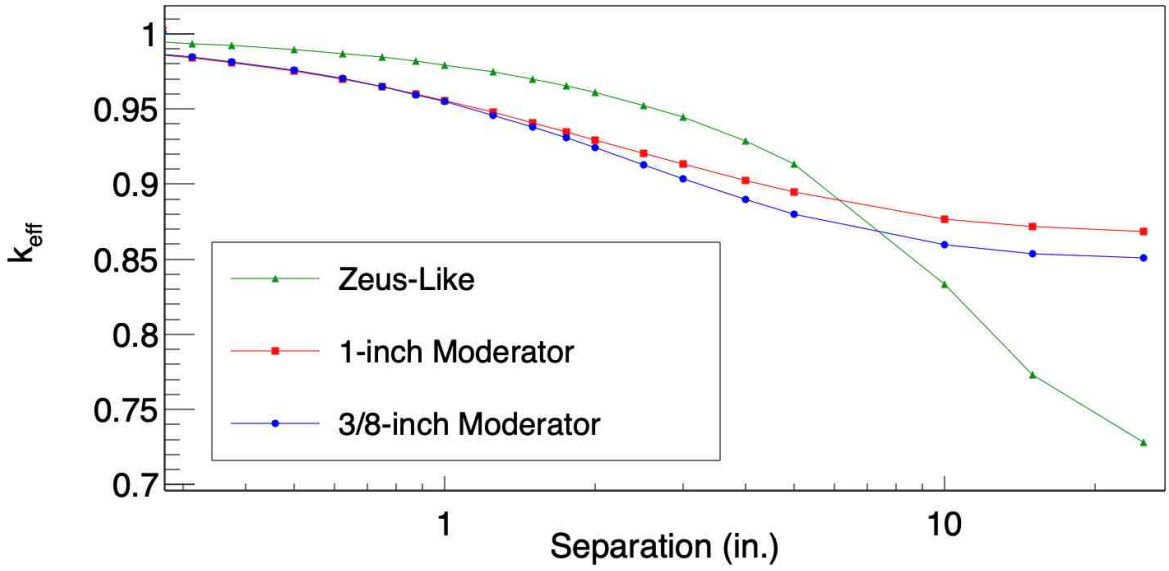

Figure 28: Separation vs k_{eff} for all of the proposed configurations.

Section 4

Conclusions

Three experimental configurations with chlorine absorbers are proposed in this final design report, with one having two variations to account for fabricability challenges to ensure that the experiment can be executed. All three of the configurations use encapsulated NaCl absorbers and the two thermal configurations use HDPE moderators. Two of the three configurations are polyethylene reflected, as typical for TEX-HEU variants, and one configuration is copper reflected, aligning with the Zeus variants. The two polyethylene reflected configurations are designed to maximize thermal sensitivity as well as maximize similarity to provided INL application case sensitivity profiles, with G parameter values as low as 0.035. The Zeus-like configuration is designed to be maximally fast, providing a larger sensitivity to the fast neutron energy region, which will provide support for MCRE, MCFR, and the uncertainty in the $^{35}Cl(n,p)$ cross section.

Of the three configurations, the two polyethylene reflected configurations utilize a ½" NaCl absorber and the copper reflected configuration has two variations, one that uses a 5/8" and on that uses a 1" NaCl absorber. All configurations utilize a standard stacking structure that repeats stacking an HEU fuel plate, a polyethylene moderator, and an absorber plate. For each of the three configurations separation distance and HEU plate swap calculations were performed to assist the approach to critical. Upper reflector thickness calculations were performed for the polyethylene reflected configurations and interstitial aluminum calculations were performed for the copper reflected configurations.

Various uncertainty calculations were performed to estimate the worth of the absorber uncertainties. These uncertainties were the absorber thickness, mass, and H_2O content. The assessment of uncertainties resulting from the absorbers was predicted to be of 0.00042 Δk_{eff}. The original TEX-Cl campaign gave insight on the impurity content, density, and moisture content of the NaCl salt. It is anticipated that the overall uncertainty on the absorber plates will be consistent with the previous experiment. The experimental uncertainties for the non-absorber components were predicted to be 0.00132 Δk_{eff}, resulting in a total uncertainty of 0.00139 Δk_{eff}.

It is expected that the NaCl absorber plates will be fabricated in half discs and assembled at Lawrence Livermore National Laboratory in similar encapsulation plates as those used in the original TEX-Cl campaign. To have an adequate amount of plates for the experiment, it is expected that we will procure, through TerraPower, up to 150 of the half discs, depending on the fabrication requirement set by the manufacturer. The procurement of these plates will be performed by TerraPower.

Procurement of any additional parts to support this experiment is not expected unless it is decided that it would be preferrable to have solid moderator plates instead of stacking plates to achieve the desired thickness.

Section 6

References

1. "*International Criticality Safety Benchmark Evaluation Project (ICSBEP*)." Nuclear Energy Agency, www.oecd-nea.org/download/science/icsbep-handbook/CD2020/.
2. J. Norris, et. al., *HEU-MET-MIXED-021, TEX-HEU Baseline Assemblies*, LLNL-TR-849789 (2023).
3. E. Aboud*, et al.*, *IER-499 CED-3b Report: TEX-Cl: Integral Experiment Execution of Thermal/Epithermal eXperiments using Highly Enriched Uranium with Polyethylene and Chloride Absorbers*, LLNL-TR-869526 (2024).
4. Amundson, K, Favorite, J.A., and Oizumi, A., *HEU-MET-FAST-102*, *ZEUS: FAST-SPECTRUM CRITICAL ASSEMBLIES WITH A Pb-HEU CORE SURROUNDED BY A COPPER REFLECTOR*, LA-UR-22-33185, Los Alamos National Laboratory: Los Alamos, NM (2023).
5. K. Casanova, *Private Communications.*
6. Norris, J., R. Araj, D.P. Heinrichs, and C. Percher, IER-297 CED-4b: *TEX-HEU Baseline Assemblies:Highly Enriched Uranium Plates with Polyethylene Moderator and Polyethylene Reflector.* 2023, Lawrence Livermore National Laboratory: Livermore, CA.
7. Nelson, A., C. Percher, W. Zywiec, and D. Heinrichs, *IER-297 CED-2: Final Design for Thermal/Epithermal eXperiments with Jemima Plates with Polyethylene and Hafnium*. 2019, Lawrence Livermore National Laboratory: Livermore, CA
8. E. Aboud, *TEX-Cl: Integral Experiment Execution of Thermal/Epithermal eXperiments using Highly Enriched Uranium with Polyethylene and Chloride Absorbers,* IER-499 CED-3b, LLNL-TR-869526, Lawrence Livermore National Laboratory: Livermore, CA (2024).
9. US Department of Agriculture (USDA), Agricultural Research Service, Nutrient Data Laboratory. USDA National Nutrient Database for Standard Reference, Legacy. Version Current: April 2018. Internet: http:/www.ars.usda.gov/nutrientdata
10. Haynes, W.M. (ed.). CRC Handbook of Chemistry and Physics, 94th Edition, CRC Press LLC, Boca Raton: FL 2013-2014, p.4-89
11. E. Aboud *et al.*, *Final Design for Thermal/Epithermal eXperiments (TEX) with Chloride Absorbers to Provide Validation Benchmarks for Y-12 Electrorefining Facility*, IER-499 CED-2, LLNL-TR-855077, Lawrence Livermore National Laboratory, Livermore, CA (2023).
12. Mosteller, R.D., R.W. Brewer, and J. Sapir, *HEU-MET-INTER-006: The Initial Set of Zeus Experiments: Intermediate-Spectrum Critical Assemblies with a Graphite-HEU Core Surrounded by a Copper Reflector*, in *International Handbook of Evaluated Criticality Safety Benchmark Experiments. NEA/NSC/DOC/(95)03/II*. 2004, Los Alamos National Laboratory: Los Alamos, NM.
13. Brewer, R., *HEU-MET-THERM-001: Polyethylene Reflected and Moderated Highly Enriched Uranium System with Silicon*, in *International Handbook of Evaluated*

Criticality Safety Benchmark Experiments. NEA/NSC/DOC/(95)03/II. 2009, Los Alamos National Laboratory: Los Alamos, NM.

Appendix A

Sample MCNP6® Input Decks

A.1 1” Moderator

1” Moderator Input Deck

A.2 3/8” Moderator

3/8” Moderator Input Deck

A.4 Zeus-Like

Zeus-Like Input Deck

Appendix B

Swapping HEU Plate Configurations

This section outlines the stacking order of the HEU plates used in the calculations of Section 3.6.2

B.1 1” Moderator Configuration

Original:

Plate Type	Name	Mass (g)
2.5-inch	B1010475	6244
2.5-inch	10464	6259
2.5-inch	10487	6277
2.5-inch	B1010470	6291
2.5-inch	B1010467	6337
solid	11149	6412
solid	11150	6441
solid	11019	6477
solid	11017	6518
solid	11147	6539
2.5-inch	B1010489	6350
2.5-inch	B1010491	6396
Total Mass		76541

Alternate Configuration 1:

Plate Type	Name	Mass (g)
2.5-inch	B1010475	6244
2.5-inch	10464	6259
2.5-inch	10487	6277
2.5-inch	B1010470	6291
2.5-inch	B1010467	6337
6-inch	B1010457	5575
solid	11150	6441
solid	11019	6477
solid	11017	6518
solid	11147	6539
2.5-inch	B1010489	6350
2.5-inch	10487	6277
Total Mass		75585

Alternate Configuration 2:

Plate Type	Name	Mass (g)
2.5-inch	B1010475	6244
2.5-inch	10464	6259
2.5-inch	10487	6277
2.5-inch	B1010470	6291
2.5-inch	B1010467	6337
6-inch	B1010457	5575
solid	11150	6441
solid	11019	6477
solid	11017	6518
10-inch	B1010463	3633
2.5-inch	B1010489	6350
2.5-inch	B1010491	6396
Total Mass		72798

Alternate Configuration 3:

Plate Type	Name	Mass (g)
2.5-inch	B1010475	6244
2.5-inch	10464	6259
2.5-inch	10487	6277
2.5-inch	B1010470	6291
2.5-inch	B1010467	6337
solid	11149	6412
solid	11150	6441
solid	11019	6477
solid	11017	6518
10-inch	B1010463	3633
2.5-inch	B1010489	6350
2.5-inch	B1010491	6396
Total Mass		73635

Alternate Configuration 4:

Plate Type	Name	Mass (g)
2.5-inch	B1010475	6244
2.5-inch	10464	6259
2.5-inch	10487	6277
2.5-inch	B1010470	6291
2.5-inch	B1010467	6337
solid	11149	6412
solid	11150	6441
solid	11019	6477
6-inch	B1010935	5444
solid	11147	6539
2.5-inch	B1010489	6350
2.5-inch	B1010491	6396
Total Mass		75467

Alternate Configuration 5:

Plate Type	Name	Mass (g)
10-inch	B1010463	3633
2.5-inch	10464	6259
2.5-inch	10487	6277
2.5-inch	B1010470	6291
2.5-inch	B1010467	6337
solid	11149	6412
solid	11150	6441
solid	11019	6477
solid	11017	6518
solid	11147	6539
2.5-inch	B1010489	6350
2.5-inch	B1010491	6396
Total Mass		73930

B.2 3/8” Moderator Configuration

Original:

Plate Type	Name	Mass (g)
6-inch	B1010935	5444
6-inch	B1010477	5511
2.5-inch	B1010475	6244
2.5-inch	10464	6259
2.5-inch	10487	6277
2.5-inch	B1010470	6291
2.5-inch	B1010467	6337
solid	11149	6412
solid	11150	6441
solid	11019	6477
solid	11017	6518
solid	11147	6539
2.5-inch	B1010489	6350
2.5-inch	B1010491	6396
Total Mass		87496

Alternate Configuration 1:

Plate Type	Name	Mass (g)
10-inch	B1010463	3633
6-inch	B1010477	5511
2.5-inch	B1010475	6244
2.5-inch	10464	6259
2.5-inch	10487	6277
2.5-inch	B1010470	6291
2.5-inch	B1010467	6337
solid	11149	6412
solid	11150	6441
solid	11019	6477
solid	11017	6518
solid	11147	6539
2.5-inch	B1010489	6350
2.5-inch	B1010491	6396
Total Mass		85685

Alternate Configuration 2:

Plate Type	Name	Mass (g)
10-inch	B1010463	3633
6-inch	B1010477	5511
2.5-inch	B1010475	6244
2.5-inch	10464	6259
2.5-inch	10487	6277
2.5-inch	B1010470	6291
2.5-inch	B1010467	6337
solid	11149	6412
solid	11150	6441
solid	11019	6477
solid	11017	6518
6-inch	B1010457	5575
2.5-inch	B1010489	6350
2.5-inch	B1010491	6396
Total Mass		84721

Alternate Configuration 3:

Plate Type	Name	Mass (g)
6-inch	B1010935	5444
6-inch	B1010477	5511
2.5-inch	B1010475	6244
2.5-inch	10464	6259
solid	11149	6412
2.5-inch	B1010470	6291
2.5-inch	B1010467	6337
solid	11149	6412
solid	11150	6441
solid	11019	6477
solid	11017	6518
solid	11147	6539
2.5-inch	B1010489	6350
2.5-inch	B1010491	6396
Total Mass		87631

Alternate Configuration 4:

Plate Type	Name	Mass (g)
6-inch	B1010935	5444
6-inch	B1010477	5511
2.5-inch	B1010475	6244
2.5-inch	10464	6259
2.5-inch	10487	6277
2.5-inch	B1010470	6291
2.5-inch	B1010467	6337
solid	11149	6412
solid	11150	6441
solid	11019	6477
10-inch	B1010463	3633
solid	11147	6539
2.5-inch	B1010489	6350
2.5-inch	B1010491	6396
Total Mass		84611

Alternate Configuration 5:

Plate Type	Name	Mass (g)
6-inch	B1010935	5444
6-inch	B1010477	5511
6-inch	B1010477	5511
2.5-inch	10464	6259
2.5-inch	10487	6277
2.5-inch	B1010470	6291
2.5-inch	B1010467	6337
solid	11149	6412
solid	11150	6441
solid	11019	6477
solid	11017	6518
solid	11147	6539
2.5-inch	B1010489	6350
2.5-inch	B1010491	6396
Total Mass		86763

B.3 Zeus-Like Configuration

Original:

Plate Type	Name	Mass (g)	Plate Type	Name	Mass (g)
10-inch	B1010463	3633	21/15	-1	6141
6-inch	B1010457	5575	21/15	-2	6149
6-inch	B1010932	5440	21/15	-3	6121
6-inch	10933	5442	21/15	-4	6120
solid	11149	6412	21/15	-5	5976
solid	11150	6441	21/15	-6	6158
solid	11019	6477	21/15	-7	6132
solid	11017	6518	21/15	-10	6155
solid	11147	6539	21/15	-11	6138
6-inch	B1010935	5444	21/15	-13	6046
6-inch	B1010477	5511	21/15	-14	6148
2.5-inch	B1011018	5378	21/15	-17	6152
2.5-inch	10464	6259	21/15	-19	6150
2.5-inch	10487	6277	21/15	-20	6177
2.5-inch	B1010470	6291	21/15	-21	6102
2.5-inch	B1010467	6337	21/15	-22	6054

2.5-inch	B1010489	6350	21/15	-23	6134
2.5-inch	B1010491	6396	21/16	-24	6095
Total Mass					216868

Alternate Configuration 1:

Plate Type	Name	Mass (g)	Plate Type	Name	Mass (g)
10-inch	B1010463	3633	21/15	-1	6141
10-inch	B1010458	3619	21/15	-2	6149
6-inch	B1010932	5440	21/15	-3	6121
6-inch	10933	5442	21/15	-4	6120
solid	11149	6412	21/15	-5	5976
solid	11150	6441	21/15	-6	6158
solid	11019	6477	21/15	-7	6132
solid	11017	6518	21/15	-10	6155
solid	11147	6539	21/15	-11	6138
6-inch	B1010935	5444	21/15	-13	6046
6-inch	B1010477	5511	21/15	-14	6148
2.5-inch	B1011018	5378	21/15	-17	6152
2.5-inch	10464	6259	21/15	-19	6150
2.5-inch	10487	6277	21/15	-20	6177
2.5-inch	B1010470	6291	21/15	-21	6102
2.5-inch	B1010467	6337	21/15	-22	6054
2.5-inch	B1010489	6350	21/15	-23	6134
6-inch	B1010457	5575	21/16	-24	6095
Total Mass					214091

Alternate Configuration 2:

Plate Type	Name	Mass (g)	Plate Type	Name	Mass (g)
6-inch	B1010457	5575	21/15	-1	6141
6-inch	B1011018	5378	21/15	-2	6149
6-inch	B1010932	5440	21/15	-3	6121
6-inch	10933	5442	21/15	-4	6120
solid	11149	6412	21/15	-5	5976
solid	11150	6441	21/15	-6	6158
solid	11019	6477	21/15	-7	6132
solid	11017	6518	21/15	-10	6155
solid	11147	6539	21/15	-11	6138
6-inch	B1010935	5444	21/15	-13	6046
6-inch	B1010477	5511	21/15	-14	6148

2.5-inch	B1011018	5378	21/15	-17	6152
2.5-inch	10464	6259	21/15	-19	6150
2.5-inch	10487	6277	21/15	-20	6177
2.5-inch	B1010470	6291	21/15	-21	6102
2.5-inch	B1010467	6337	21/15	-22	6054
2.5-inch	B1010489	6350	21/15	-23	6134
2.5-inch	B1010491	6396	21/16	-24	6095
Total Mass					218613

Alternate Configuration 3:

Plate Type	Name	Mass (g)	Plate Type	Name	Mass (g)
10-inch	B1010463	3633	21/15	-1	6141
10-inch	B1010458	3619	21/15	-2	6149
6-inch	B1010932	5440	21/15	-3	6121
6-inch	10933	5442	21/15	-4	6120
solid	11149	6412	21/15	-5	5976
solid	11150	6441	21/15	-6	6158
solid	11019	6477	21/15	-7	6132
solid	11017	6518	21/15	-10	6155
solid	11147	6539	21/15	-11	6138
6-inch	B1010935	5444	21/15	-13	6046
6-inch	B1010477	5511	21/15	-14	6148
2.5-inch	B1011018	5378	21/15	-17	6152
2.5-inch	10464	6259	21/15	-19	6150
2.5-inch	10487	6277	21/15	-20	6177
2.5-inch	B1010470	6291	21/15	-21	6102
2.5-inch	B1010467	6337	21/15	-22	6054
6-inch	B1011018	5378	21/15	-23	6134
6-inch	B1010457	5575	21/16	-24	6095
Total Mass					213119

Alternate Configuration 4:

Plate Type	Name	Mass (g)	Plate Type	Name	Mass (g)
10-inch	B1010463	3633	21/15	-1	6141
6-inch	B1010457	5575	21/15	-2	6149
6-inch	B1010932	5440	21/15	-3	6121
6-inch	10933	5442	21/15	-4	6120
solid	11149	6412	21/15	-5	5976
solid	11150	6441	21/15	-6	6158

solid	11019	6477	21/15	-7	6132
solid	11017	6518	21/15	-10	6155
solid	11147	6539	21/15	-11	6138
6-inch	B1010935	5444	21/15	-13	6046
6-inch	B1010477	5511	21/15	-14	6148
2.5-inch	B1011018	5378	21/15	-17	6152
2.5-inch	10464	6259	21/15	-19	6150
2.5-inch	10487	6277	21/15	-20	6177
2.5-inch	B1010470	6291	21/15	-21	6102
2.5-inch	B1010467	6337	21/15	-22	6054
2.5-inch	B1010489	6350	21/15	-23	6134
6-inch	B1010457	5575	21/16	-24	6095
Total Mass					216047

Alternate Configuration 5:

Plate Type	**Name**	**Mass (g)**	**Plate Type**	**Name**	**Mass (g)**
10-inch	B1010463	3633	21/15	-1	6141
10-inch	B1010458	3619	21/15	-2	6149
6-inch	B1010932	5440	21/15	-3	6121
6-inch	10933	5442	21/15	-4	6120
solid	11149	6412	21/15	-5	5976
solid	11150	6441	21/15	-6	6158
solid	11019	6477	21/15	-7	6132
solid	11017	6518	21/15	-10	6155
solid	11147	6539	21/15	-11	6138
6-inch	B1010935	5444	21/15	-13	6046
6-inch	B1010477	5511	21/15	-14	6148
2.5-inch	B1011018	5378	21/15	-17	6152
2.5-inch	10464	6259	21/15	-19	6150
2.5-inch	10487	6277	21/15	-20	6177
2.5-inch	B1010470	6291	21/15	-21	6102
2.5-inch	B1010467	6337	21/15	-22	6054
6-inch	B1011018	5378	21/15	-23	6134
6-inch	B1010457	5575	21/16	Aluminum	-
Total Mass					207024

Appendix C

Final Design Stacking Configurations

This section shows the stacking orientation for the identified configurations. The outer reflector is only shown on the top, bottom, and one side even though in reality it completely surrounds the core.

C.1 1” Moderator Configuration

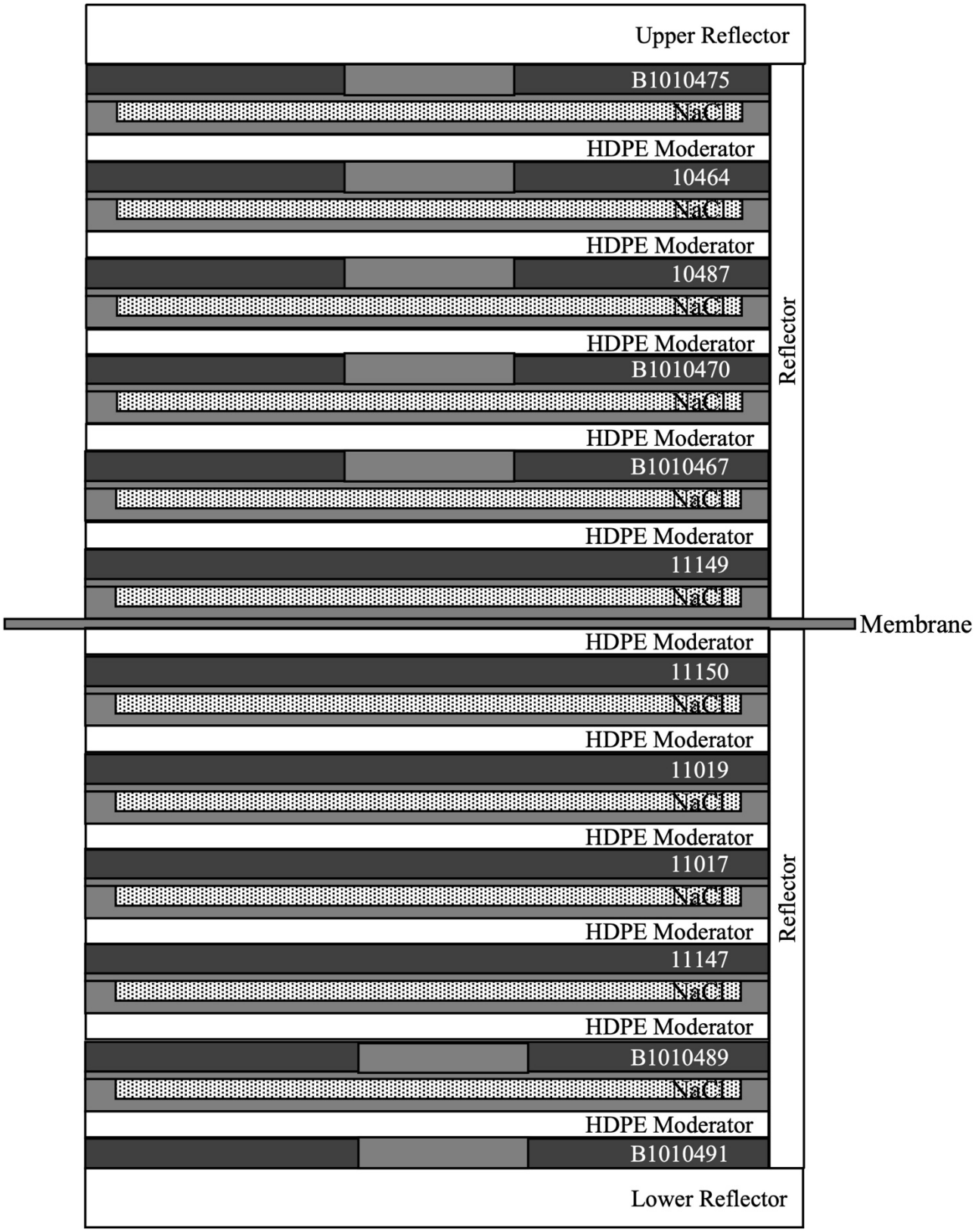

C.2 3/8” Moderator Configuration

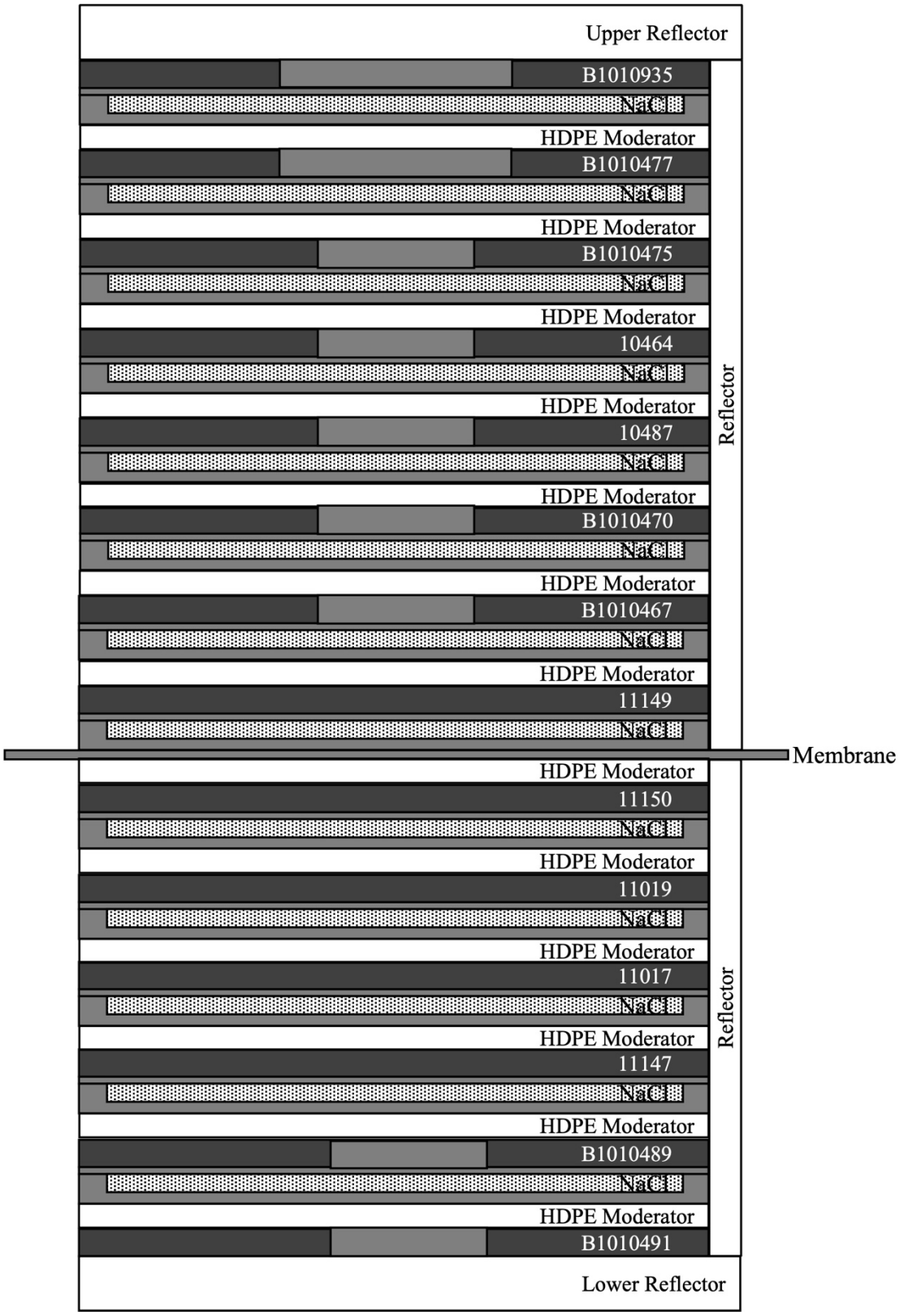

C.3 Zeus-Like Configuration

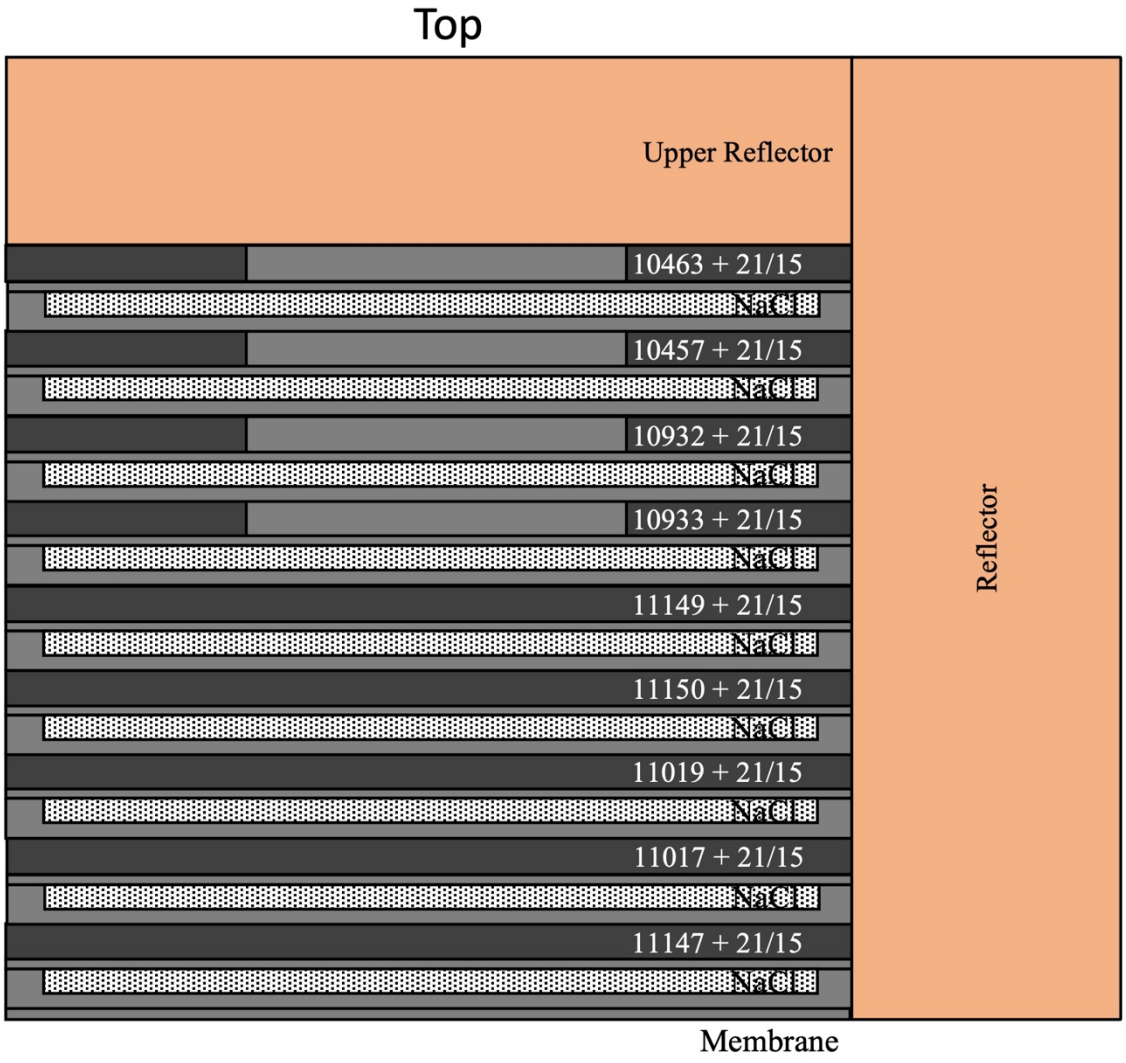

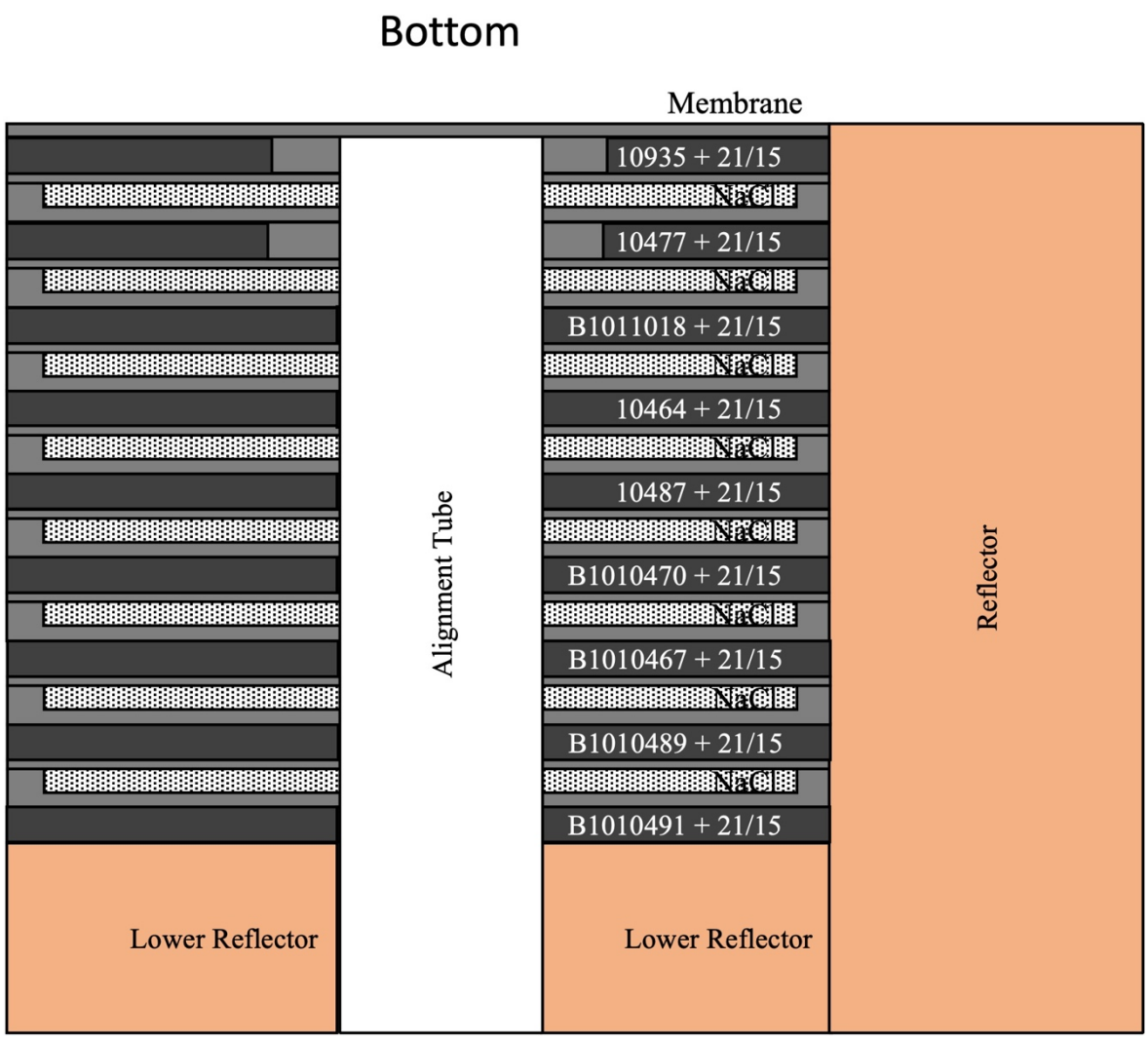
Bottom
Membrane
10935 + 21/15
NaCl
10477 + 21/15
NaCl
B1011018 + 21/15
NaCl
10464 + 21/15
NaCl
10487 + 21/15
NaCl
B1010470 + 21/15
NaCl
B1010467 + 21/15
NaCl
B1010489 + 21/15
NaCl
B1010491 + 21/15
Alignment Tube
Reflector
Lower Reflector
Lower Reflector

Appendix D

Copper Sheath Design

D.1 Design Results

Two copper reflected configurations were identified: one that uses a central alignment tube and one that utilizes a copper reflector sleeve around the 15" HEU plates to perform alignment. This is to account for possible manufacturing challenges, which allows us to select either if the manufacturing process becomes more advantageous than the other. The copper sleeve, which is less preferable from an operational standpoint, will be presented here.

Table 27 and Table 28 display the physical and neutronics parameters for the Zeus-like copper reflected configuration model, respectively. This configuration is predicted to have 18 fuel layers.

Table 27: Physical characteristics for the selected standard stacking configurations.

Number of Layers	HDPE Moderator Thickness (in)	NaCl Absorber Thickness (in)	HEU Mass (g)	H/D Ratio
18 – Cu Ring	-	5/8"	109,331	1.07

Table 28: Neutronics characteristics for the selected standard stacking configurations. Statistical uncertainty in k_{eff} for both models is at 0.00007.

Number of Layers	k_{eff}	k_{eff} of Half Stack	Maximum Thermal Capture Sensitivity Amplitude	Maximum Fast Capture Sensitivity Amplitude	Minimum G Parameter for INL	Thermal Fission Fraction (%)	Intermediate Fission Fraction (%)	Fast Fission Fraction (%)
18 – Cu Ring	1.00178	0.72373	-	0.0076	0.155	0.00	28.51	71.49

The sensitivity profile is compared to the Idaho National Laboratory / TerraPower application case sensitivity profiles in, introduced in Section 1, shown in Figure 29. Included in the sensitivity profile plot is the corresponding residuals which are simply the deviation of the application case profiles to that of the proposed configuration. This configuration is predominantly fast, providing sensitivity to the fast bump in the INL/TerraPower profiles as well as validation for the $^{35}Cl(n,p)$ cross section. Figure 30 shows the fission fractions per unit lethargy for the configuration.

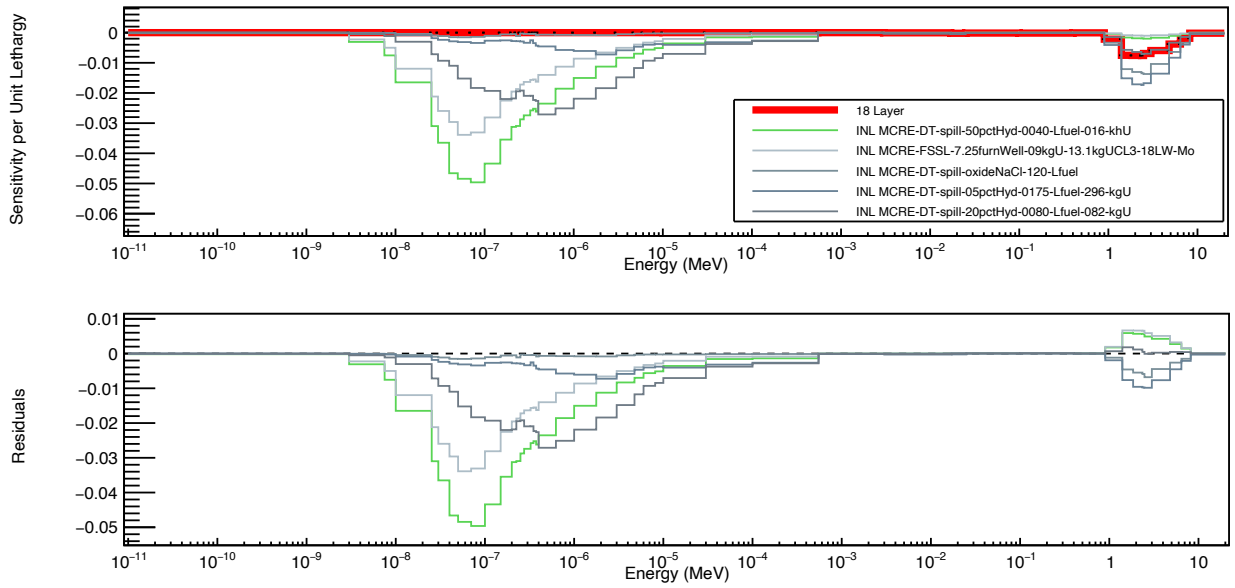

Figure 29: Neutron capture sensitivity profile for the Zeus-like configuration with the copper alignment ring compared to the INL application case sensitivity profiles.

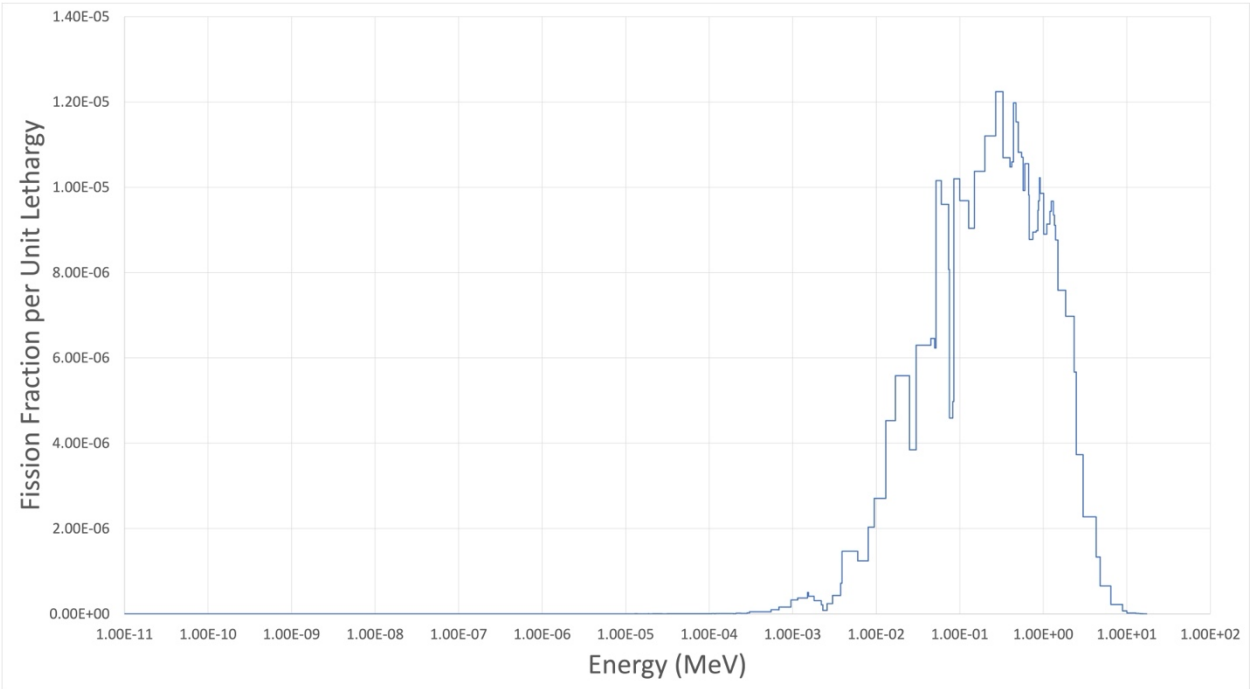

Figure 30: Fission fraction per unit lethargy for the Zeus-like configuration with the copper alignment ring.